US Army Corps of Engineers©

Performance Evaluation of the New Orleans and Southeast Louisiana Hurricane Protection System

Draft Final Report of the Interagency Performance Evaluation Task Force

Volume VIII – Engineering and Operational Risk and Reliability Analysis

1 June 2006

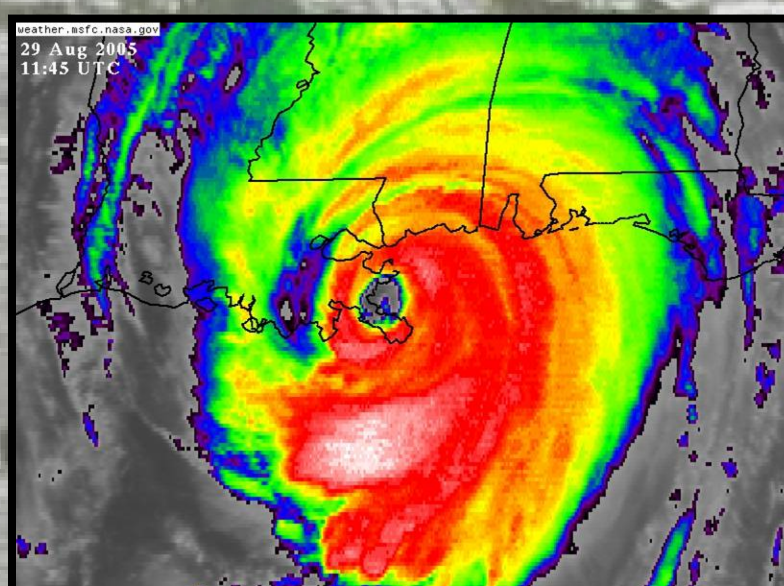

FINAL DRAFT

(Subject to Revision)

Volume VIII
Engineering and Operational Risk and Reliability Analysis

This report is not intended as a final expression of the findings or conclusions of the United States Army Corps of Engineers, nor has it been adopted by the Corps as such. Rather, this is a preliminary report summarizing data and interim results compiled to date. As a preliminary report, this document and the information contained therein are subject to revisions and changes as additional information is obtained.

Contents

Executive Summary

The mission of the Interagency Performance Evaluation Task Force (IPET) risk and reliability analysis was to examine the risks to life and property posed by the New Orleans hurricane protection system (HPS) that was in place prior to Katrina and by the system as it is expected to exist at the start of the next hurricane season (1 June 2006). The purpose of the analysis was to identify areas of the HPS that are relatively more vulnerable to flooding than others, and to identify the sources of that vulnerability. The studies also provide estimates of the frequency of flooding within each drainage basin. By examining the pre- and post-Katrina risks, the effectiveness of the repairs and improvements made to the HPS since Katrina can be evaluated. The risk analysis considered the expected performance of the various elements of the system and the consequences associated with that performance. This report outlines the procedures and methodologies used in the risk studies. The results of the risk analysis are undergoing review and validation and will be published subsequent to a full peer review.

The risk analysis covers four postulated states of the New Orleans HPS:

1. The system as it existed before the arrival of Hurricane Katrina. Knowledge gained from IPET studies was considered in the analysis.

2. Following Hurricane Katrina with repairs that have been completed prior to the 2006 hurricane season. Some projects may be ongoing after 1 June 2006.

3. Following Hurricane Katrina with all repair and improvement projects complete, but prior to longer term increases in the authorized level of protection.

4. The system as authorized before the arrival of Hurricane Katrina. All authorized components of the HPS are constructed and knowledge gained from IPET studies was considered in the analysis.

Conditions 3 and 4 have not been completed prior to the submittal of the final IPET report. The difference in relative risks among the these states was a unified measure for fully evaluating the performance of the integrated system before Hurricane Katrina, after Hurricane Katrina, and during the interim recovery period.

Two groups of questions concerning the performance of the HPS are addressed by the risk and reliability analyses:

Group 1 - Pre-Katrina: The system as it existed before the arrival of Hurricane Katrina. This state is the baseline for estimating risk and includes the following:

1. What was the estimated reliability of the HPS that was in existence before the arrival of Katrina in preventing flooding of protected areas of the HPS that was in existence before the arrival of Katrina, for the range of hurricanes expected to impact New Orleans? Note that some components of the authorized projects had not been constructed prior to Katrina so only the features in place are considered in this scenario.

2. What would have been the reliability of the HPS in preventing flooding of protected areas for the range of hurricanes expected to impact New Orleans if the entire authorized project had been completed?

3. What is the estimated annual rate of occurrence of system failure due to the range of expected hurricane events?

4. What are the probabilities and annual rates of occurrence of consequences that would result from failure of the HPS as defined in terms of life loss and economic impact?

5. What is the uncertainty in these estimates?

Condition 2 has not been completed prior to the submittal of the final IPET report. The pre-Katrina risk analysis does not attempt to recreate the design intent or knowledge that the designers used to determine the configuration of the HPS. Engineering parameters, foundation conditions, and operational information gained by IPET through exploration and testing since the hurricane are used. This allows for an estimate of the risks that existed pre-Katrina. An additional analysis was conducted on the authorized HPS that includes all features in the original design that were not completed prior to Katrina.

Group 2 - Post-Katrina: After Hurricane Katrina with repairs made prior to the 2006 hurricane season, and during the interim recovery period after the hurricane protection system has been strengthened and improved, but prior to longer term increases in the authorized level of protection. This group includes:

1. What is the reliability of the HPS with regard to preventing flooding of protected areas for the range of hurricanes expected to impact New Orleans with the system repairs and improvements in place as of 1 June 2006?

2. What is the frequency of flooding due to the range of expected hurricane events with the system repairs and improvements in place as of 1 June 2006?

3. What are the probability distributions of consequences, defined in terms of life loss and economic impact, and their annual rates of consequences that would result from failure of the HPS?

4. What is the uncertainty in these estimates?

The condition of the system has been degraded by the effects of Hurricane Katrina. Flood walls and levees may have been overtopped, damaged by impacts from debris, saturated, submerged, and/or breached. Permanent repairs on these elements have been accomplished since the hurricane using materials and components that may have different strength parameters than the original features. This difference in strengths is considered in the analyses of component reliability. The pumping system was also damaged and shut down or submerged. The post-Katrina reliability of the levees, flood wall, and pumping stations was considered in the risk assessment. The reliability of the various elements of the protection system was determined using analytical and expert elicitation methods.

The term “reliability” is intended to mean the conditional probability of a component or system performing an intended function given that a specific hurricane surge has occurred. This result can also be used to determine the conditional probability of failure. System failure refers to the failure of the HPS to provide protection from flooding in one or more protected areas and can also be thought of as the occurrence of flood inundation. The effectiveness of the protection system is also dependent upon how well the operational elements of the system performed. Elements such as road closure structures, gate operations and pumping plants, etc., that require human operation and proper installation during a flood fight can dramatically impact flood levels. The lessons learned concerning the performance of these elements during Katrina was considered in the analysis.

The changed demographics of the local areas protected by the system were considered when determining the consequences. In some areas, many homes and much of the infrastructure were destroyed by the hurricane and some may not be rebuilt. Therefore, the pre-Katrina populations and property values were impacted and must be considered in the post-Katrina analysis. The Consequence Team has provided the estimated post-Katrina direct economic damage and population projections that are used in the risk analysis.

“Risk” is defined as expected losses in terms of lives or dollars generally calculated by combining the probability of system failure with the consequences associated with that failure. For New Orleans, the post-Katrina risks were different due to the changing demographics noted above. In order to better compare the adequacy of the pre- and post-Katrina HPS, probability of failure and frequency of inundation mapping were used as the primary metrics by which to measure the effectiveness of repairs and improvements. The inundation mapping, and associated stage-frequency curves, are intended to be used for estimating the relative risks of flooding throughout the New Orleans area for the purpose of identifying areas of vulnerability. These estimates should not be compared to inundation mapping conducted under the Federal Emergency Management Agency’s (FEMA’s) flood insurance programs since the methods of analyses, ADCIRC grids, and number of hurricanes modeled are different. The Risk Team has coordinated with FEMA during the analyses to identify similarities and differences in the methods of analysis.

Participants

The following individuals actively participated on this project during the period October 2005 through June 2006.

Name	**Agency**	**Role**
Co-Leads		
Jerry L. Foster, P.E.	HQUSACE	Lead Project Coordinator & Manager
Bruce Muller, P.E.	USBR	Asst. Project Coordinator
Headquarters		
Donald R. Dressler, P.E	HQUSACE	Project Sponsor

Anjana Chudgar	HQUSACE	Project Monitor
Team Members		
Bilal M. Ayyub, PhD, PE,	University of Maryland	Lead Risk Analysis Model Developer
Gregory Baecher, PhD.	University of Maryland	Geotechnical Reliability
Brian Blanton	University of North Carolina	ADCIRC modeler
David Bowles, PhD	RAC Engineers	Consequences
Jennifer Chowning	USACE – LRL	GIS Mapping
Robert Dean, PhD	U of Fla	Wave Modeler & Coastal Engineering
David Divoky	Watershed Concepts	Lead Hurricane Modeling
Bruce Ellingwood, PhD	Georgia Institute of Technology	Technical Review
Richalie Griffith	USACE – NAE	GIS mapping
Wayne Jones, P.E.	ERDC-ITL	Program Manager & System Definitions
Mark Kaminskiy, PhD	University of Maryland	Risk Methodology
Burton Kemp	New Orleans District (retired)	Field Geologist
Fred Krimgold, PhD	Virginia Tech	Consequences
Therese McAllister, PhD	NIST	Reliability & Technical Review
Marty McCann, PhD	Stanford University	Uncertainty Analysis
William McGill, PE	University of Maryland	Risk Modeler
Robert Patev, P.E.	New England District, USACE	Lead Geotechnical and Reliability
David Schaaf, P.E.	USACE - LRL	Reliability and System Definition
Terry Sullivan, P.E.	USACE-LRL	Field Surveys
Pat Taylor	ERDC- GSL	Field Surveys
Nancy Towne	ERDC- ITL	GIS Mapping
Daniele Veneziano, PhD	MIT	Hurricane Modeling
Greg Walker	Contractor, ERDC-ITL	Programmer
Mathew Watts	USACE – LRL	Field Surveys
Allyson Windham	ERDC-ITL	GIS Mapping

Background

All civil engineering systems impose risks that result from humans using technology in an attempt to control naturally occurring conditions. For instance, the hurricane protection system in New Orleans has been designed to provide protection from storm induced surges and waves. An interior drainage system controls flooding within the city during normal rainfall and tropical storm events. The hurricane protection system (HPS) project was designed to perform this function without imposing unacceptable risks to public safety, property and welfare.

The term "risk" is used many ways to define hazards, losses, potential problems, etc. In the civil engineering community, risk is generally defined as the rate that lives, economic, environmental, and social/cultural losses will occur due to the performance of an engineered system or component. The performance is defined as the probability that specific loads will cause the system to fail and losses are defined as the adverse impacts of that failure if it occurs. In simplified mathematical terms:

$$\text{Risk} = \text{Probability of Failure} \times \text{Consequences of Failure}$$

This simple equation not only defines risk but also shows that there are two ways to control or mitigate risks: by making the system more reliable or by reducing the potential losses during a failure. The probability of failure part of the equation was influenced by engineers by strengthening of existing structures or by adding additional protection; however the consequence part is highly dependent upon the actions and decisions made by residents, government and local officials. In densely populated areas, simply increasing system reliability may not reduce risks to acceptable levels and increasing consequences through continued flood plain development can offset any risk gains.

Decisions concerning investments in systems designed to control natural hazards are best made by explicitly and quantitatively considering the risks that the systems will pose to public safety and property. Implementation of risk analysis to the HPS of New Orleans and S.E. Louisiana is difficult because it is a complex system of levees, floodwalls and pumping stations that serves a large geographical region. In addition, our capability to accurately predict and model hurricanes in regions as complex as the Mississippi delta is limited. Nonetheless, mathematical modeling of hurricanes and risk analysis methodologies have improved enough in recent years to make risk analysis an important tool for investment decision making as the New Orleans HPS is restored and improved.

The reliability and risk analyses relate the performance of individual features (floodwalls, levees, pumps, levee closures, etc.) located throughout the hurricane protection system to the overall performance of the integrated system and the impact of that performance on public safety and, social and economic welfare. The reliability of the various features also considers the varying material properties of the structures and of foundation conditions that exist throughout the hurricane protection system.

It is important to note that detailed knowledge of the engineering parameters that influence the performance of the HPS and of the hurricane characteristics of storms expected to impact

New Orleans is limited. For example, we do not know with certainty the properties of foundation soils underlying every section of the extensive levee and floodwall system, or even the frequency with which hurricanes will occur in the future. Hurricane models can predict winds, waves and surges only with limited precision, and the reliability models used to predict levee performance when subjected to hurricane forces are similarly limited. Hence, the risks of hurricane-induced flooding cannot be established with certainty. Therefore a risk analysis must include not just a best estimate of risk, but also an estimate of the uncertainty in that best estimate. By identifying the sources of uncertainty in the analysis, measures such as gathering additional data was taken to reduce the uncertainty and improve the risk estimates.

The IPET risk analysis considers two states that represent the condition of the New Orleans HPS.

- The system as it existed before the arrival of Hurricane Katrina. This state is the baseline for estimating risk.
- The system following Hurricane Katrina with repairs made prior to the 2006 hurricane season...

Information collected and studies conducted during the IPET studies were used in the analysis of these two conditions. It is also important to note that the risk analysis of the pre-Katrina system is not intended to be a hind cast of the risks that the original design posed. The Katrina experience provides the best hind cast of risks associated with the HPS as it existed prior to Katrina, i.e., we know what occurred so the risks were high. The pre-Katrina analyses are used as the base case against which HPS improvements are measured.

Reliability analyses evaluate the performance of the various elements of the system by predicting the probabilities of failure of the elements under expected loads. The consequences associated with that performance when coupled with the probabilities of failure provides a measure of the corresponding risks. The reliability of the various elements of the protection system is determined using analytical and expert elicitation methods.

Several key considerations and characteristics of the risk studies are important to note:

- Defining the physical features of the system required an accurate inventory of all components that provide protection against storm surge and waves. It was important to model not only the cross sections and strength parameters of these components but also transitions between elements, differences in the crest elevations along a reach of similar components and varying foundation conditions. The characterization of the physical features of the protection system was, however, limited by the available information and the resources available to conduct field surveys, and process the information under IPET. These limitations are expressed in the analyses as uncertainties that are characterized and communicated so that they were accounted for in decisions making.
- The hurricane modeling and reliability analyses required an accurate depiction of the elevations of the tops of levees and walls that make up the HPS. The Risk Team developed this information from various sources as discussed herein.

- At many locations, the hurricane protection system was degraded by Hurricane Katrina. Levees and floodwalls was overtopped or otherwise damaged. The impact of these events upon the condition of the features is not necessarily apparent by visual inspection. The possibility of such weakening has been considered in the current condition of features of the system that survived Katrina in order to estimate the risk for the 2006 hurricane season.
- Emergency repairs of breached elements were accomplished after Hurricane Katrina, and permanent repairs have subsequently been completed. The structural/geotechnical strength of the repairs has been considered.
- The pumping system is an important element that controls flooding during and after a storm. Pumping plant reliability and capacity has therefore been considered.
- The consequences of pre- and post-Katrina flooding are different due to changes in population and economic activity. The Risk Team has relied on the Consequence Team to define post-Katrina exposure scenarios and to quantify the consequences of HPS failures.
- The effectiveness of the protection system depends on human factors as well as engineered systems (e.g., timely road and railroad closures, gate operations, functioning of pumping stations, and so on). Lessons learned from Katrina and other natural disasters were used in modeling the closures.

Appendix 1 lists key terminology and definitions used in this report.

Analysis Boundaries

An important initial step in the analysis is to clearly define the bounds of the study and the physical descriptions of the various components of the HPS. These bounds included defining the geographic bounds of the study region and the elements of the hurricane protection system, the resolution of information and analyses to be performed, and analysis constraints or assumptions associated with the risk and reliability analyses.

Study Region and Hurricane Protection System

The analysis examines risks to New Orleans area associated with the performance of the hurricane protection system (HPS). Figure 1 identifies the region considered and the major features of the hurricane protection system. The following basins were considered:

Orleans West Bank (OW)
New Orleans East (NOE)
Orleans Main (OM)
St. Bernard (SB)
Jefferson East (JE)
Jefferson West (JW)
Plaquemines Area (PLAQ)
St. Charles (ST)

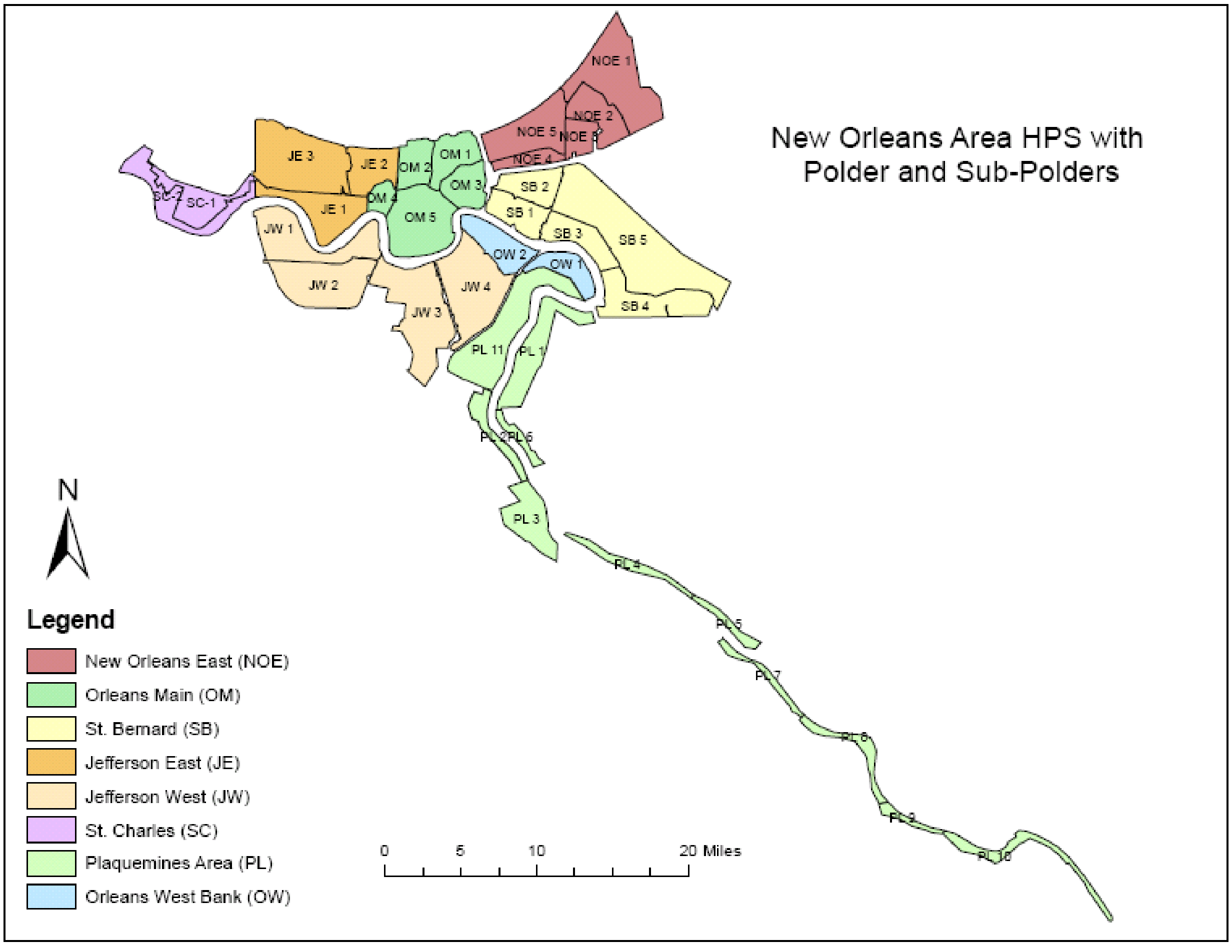

Figure 1. Map of the New Orleans and the South East Louisiana Area, the Geographic Bounds of the Study Region Considered in the Risk Analysis and the Primary Features of the Hurricane Protection System

Physical Description of the HPS

The hurricane protection system is comprised of a variety of subsystems, structures and components which include: earthen levees, floodwalls, foundation conditions, pumping stations, canals, wall closures, power supply systems, and operations personnel. The system is a combination of low-lying tracts of land that form artificial hydrologic entities enclosed by levees, called basins, which are independently maintained and operated by local parishes and levee boards.

The Risk team has developed detailed physical descriptions for each basin based on current conditions as shown in Appendices 2 through 7. Data collected by other IPET Teams, and during site inspections were used to define characteristics of the basins and their interdependence for use in the risk model. This was a critical and time consuming step in the development of the risk model that has yielded a comprehensive description of the HPS. These descriptions were developed by examining available information gathered by IPET including:

– Design memorandums and supporting documents
– Construction documents
– Inspection reports
– Katrina damage reports
– Detailed field surveys conducted by the Risk Team to verify the location and configurations of the HPS.

The information gathered was incorporated into detailed GIS based maps of each basin that included: locations of all features (Walls, levees, pumping stations, closure gates, etc.), geo-technical information (boring logs, geologic profiles), aerial photographs and photos of each feature. Appendixes 2 through 7 contain a complete inventory of the structures, systems and components of each basin that were considered in the risk analysis. The reader should note that not all of the structures, systems and components listed have been individually considered in the risk analysis model. Some items may have been combined, whereas others may not have been included since they do not play a role in the performance of the hurricane protection system or the consequences that result in the event of a failure.

For definition of the post-Katrina HPS analyses, the Risk team has coordinated with Task Force Guardian (TFG) to monitor the improvements that are expected to be in-place on 1 June 2006. These improvements include: placement of temporary closures at the end of the drainage canals, replacing I-wall with T-walls in some areas, repairs to breached sections of the HPS, and other measures as outlined in the basin descriptions.

Analysis Assumptions and Constraints

As part of the process of developing the risk analysis model, it was necessary to identify key assumptions and analysis constraints. Constraints refer to events or factors that were not modeled or considered explicitly in the analysis. The assumptions and constraints are provided at the appropriate location in subsequent sections.

The following table lists the analysis limitations or constraints of the risk analysis.

No.	Limitation or Constraint
1.	Modeling procedures that existed prior to Katrina were used.
2.	Geographic area was limited to elements of the hurricane protection system in the basins listed.
3.	The risk model does not produce temporal profiles, but spatial profiles accumulated over the entire durations of respective storms
4.	The risk model includes assumptions in various major aspects of this of the hurricane protection system characterization, hurricane simulation, reliability analysis inundation analysis, and consequence analysis
5.	Hazards and thus consequences not considered in the risk analysis are: a. Wind Damage to buildings b. Fire c. Civil unrest d. Indirect economic consequences e. Effect of a release of hazardous materials f. Environmental consequences
6.	The performance of the evacuation plan New Orleans was not explicitly modeled in the risk analysis. Evacuation effectiveness is however considered in the consequence analyses.

Risk Analysis Methodology

Overview

The following sections describe the overall risk analysis methodology of the hurricane protection system. Sections that follow discuss individual parts of the analysis as they relate to the overall risk analysis methodology. The basic elements of the risk analysis methodology are illustrated in Figure 2. The analysis is represented in terms of a series of modules which interface to provide a risk model for the New Orleans HPS. Details specific to the risk methodology are provided in Appendix 9.

Contributing Factors and Their Relationships

The development of the risk analysis model was facilitated by the preparation of an influence diagram. The process of creating an influence diagram helped establish a basic understanding of the elements of the hurricane protection system and their relationship to the overall system performance during a hurricane event and the analysis of consequences and risks.

Figure 3 shows the influence diagram for the hurricane protection system and the analysis of consequences. There are four parts to the influence diagram:

- Value nodes (rounded-corner box)
- Chance nodes (circular areas)
- Decision nodes (square-corner boxes)
- Factors and dependencies in the form of arrows.

The influence diagram shown in Figure 3 was used to develop an event (or probability) tree for the hurricane protection system. Figure 4 shows an initial probability tree derived from the influence diagram in Figure 3. The top events across the tree identify the random events whose performance during and immediately after the hurricane could contribute to flooding in a protected area. The tree begins with the initiating event, a hurricane that generates a storm surge, winds and rainfall in the region.

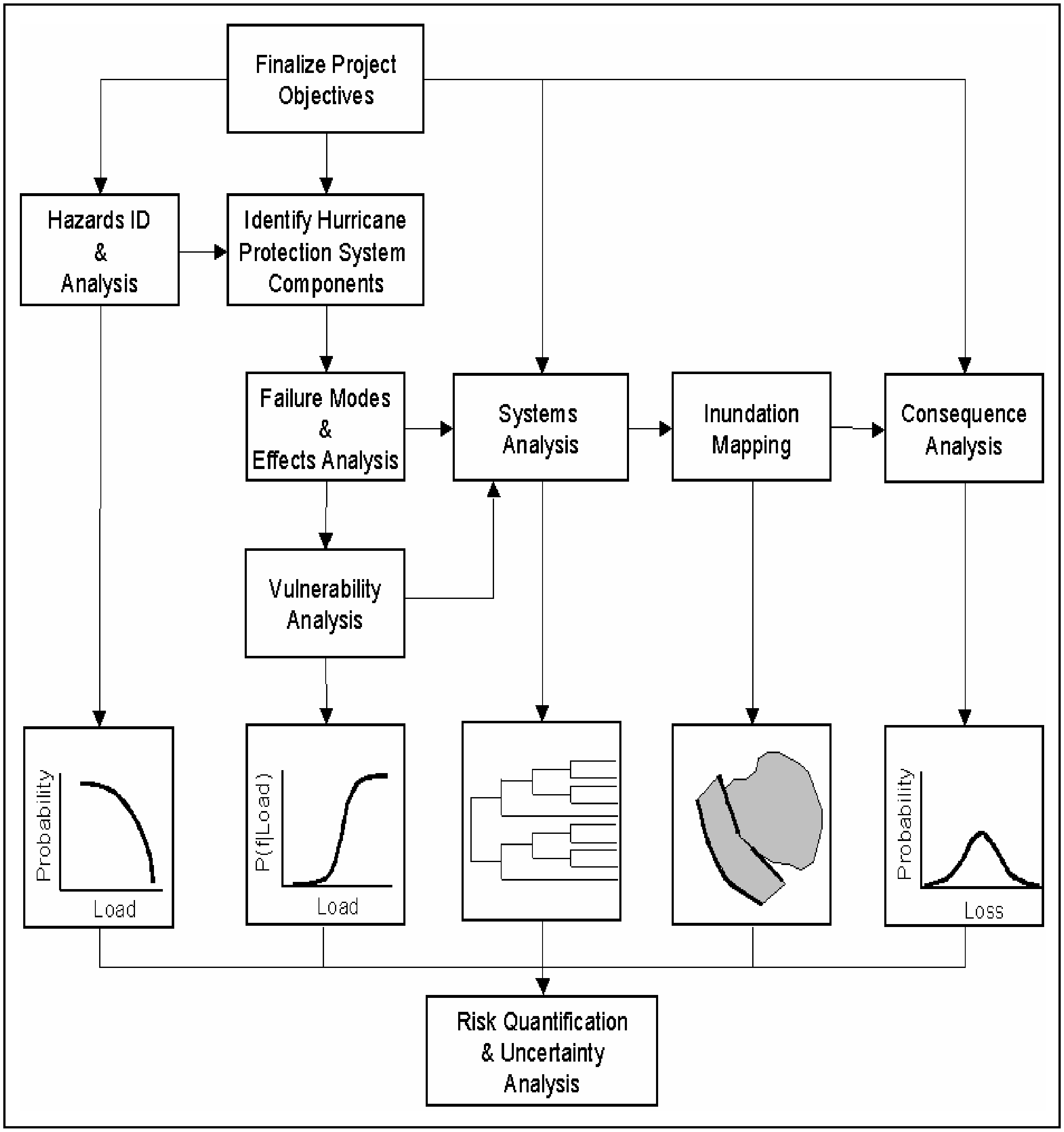

Figure 2. Risk Analysis Logic Diagram

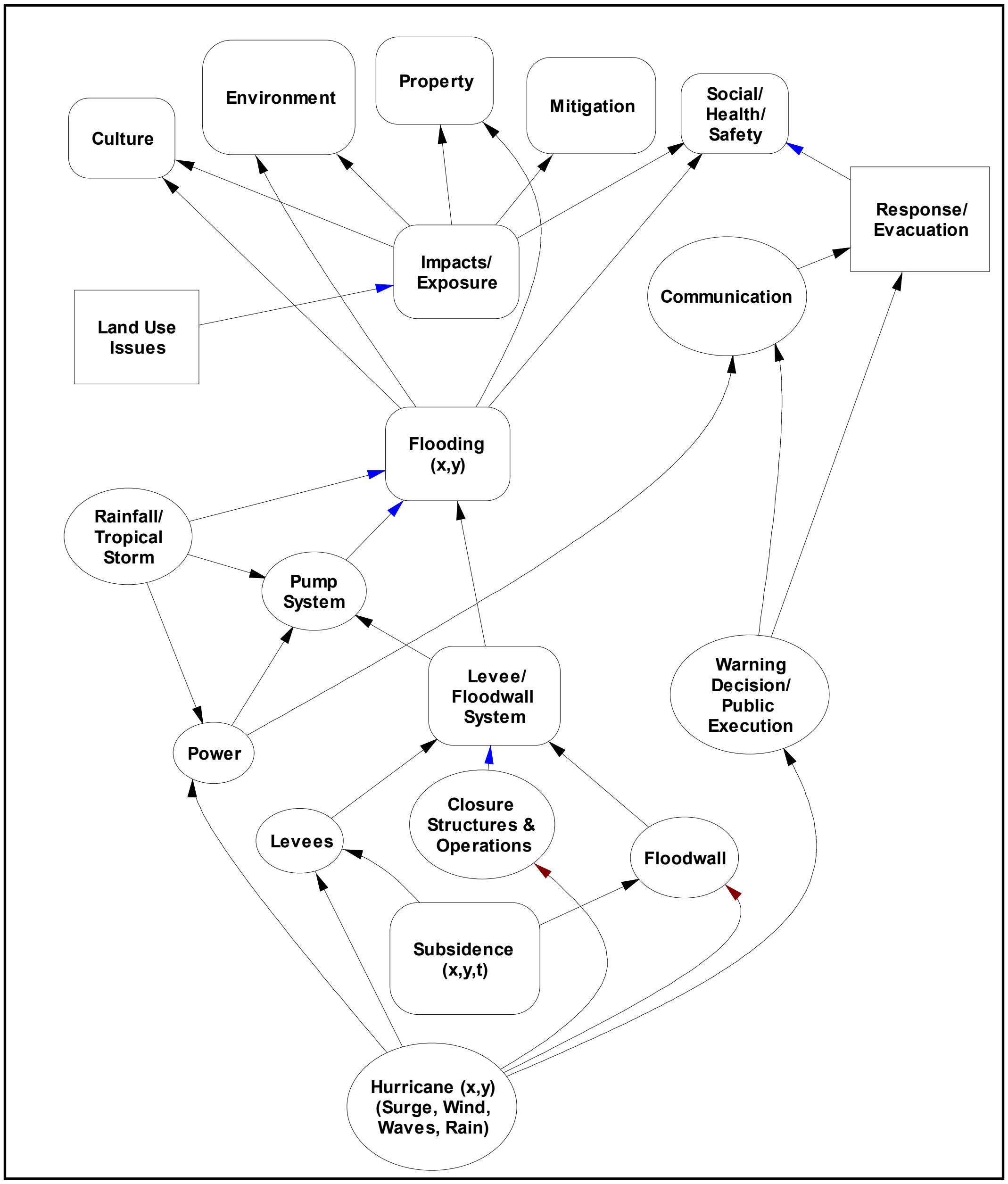

Figure 3. Influence Diagrams for Risk Analysis

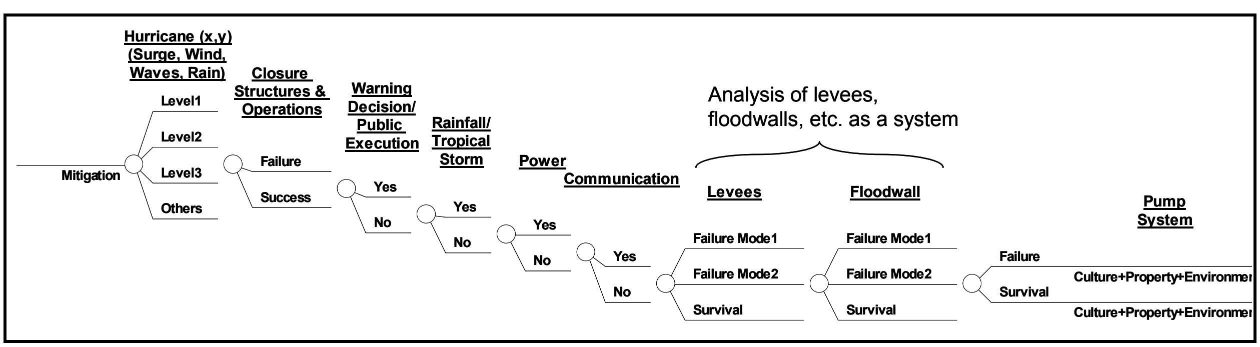

Figure 4. Probability Tree for the Hurricane Protection System

Hurricane Protection System Definition

The hurricane protection system (HPS) for the New Orleans metropolitan area is provided in Figure 1. The HPS information included in the system descriptions described above have been discretized for the reliability and risk analysis tasks as schematically shown in Figure 5. The system consists of basins, subbasins and reaches. The definition of these basins, subbasins and reaches are based on the following considerations:

- Local jurisdiction,
- Floodwall type and cross section,
- Levee type and cross section,
- Engineering parameters defining structural performance,
- Soil strength parameters,
- Foundations parameters, and

Reaches (*R*) of each basin are uniquely identified using sequential numbers illustrated in the Figure 5. The figure also shows the approximate locations of pumping stations for the purpose of illustration. Detailed maps and descriptions of each basin are provided in Appendices 2 through 7.

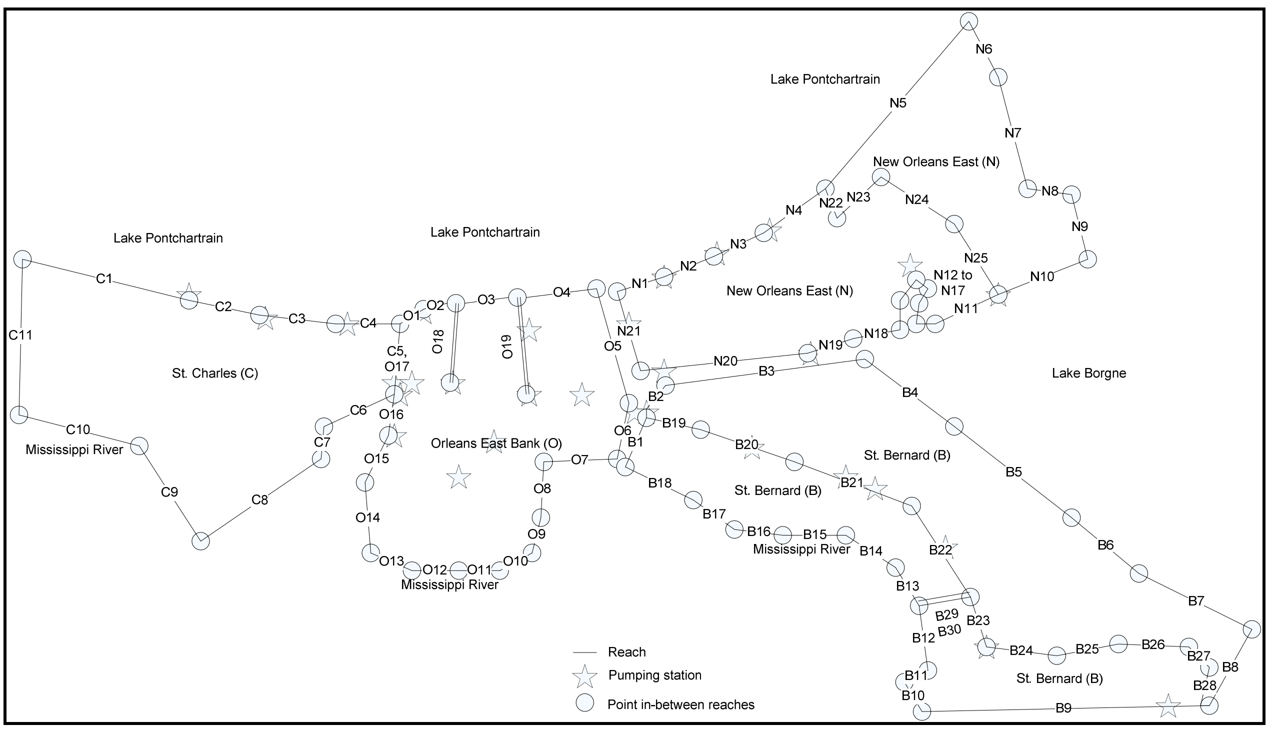

Figure 5. Hurricane Protection System Defined by Basins and Reaches

Probabilistic Risk Model

Risk associated with the hurricane protection system is quantified through a regional hurricane rate (λ) and the probability $P(C > c)$ with which a consequence measure (C) exceeds different levels (c). The loss exceedance probability per event is evaluated as

$$P(C > c) = \sum_i \sum_j P(h_i) P(S_j \mid h_i) P(C > c \mid h_i, S_j) \quad (1)$$

An annual loss exceedance rate was estimated as follows

$$\lambda(C > c) = \sum_i \sum_j \lambda P(h_i) P(S_j \mid h_i) \times P(C > c \mid h_i, S_j) \quad (2)$$

Where $P(h_i)$ is the probability of hurricane events of type i, $P(S_j|h_i)$ is the probability that the system is left in state j from the occurrence of h_i, and $P(C > c \mid h_i, S_j)$ is the probability that the consequence C exceeds level c under (h_i, S_j). Summation is over all hurricane types i and all system states j in a suitable discretization. Simulation studies of hurricanes for risk analysis require the use of representative combinations of hurricane parameters and their respective probabilities. The outcome of this process is a set of hurricane simulation cases and their respective conditional rates $\lambda P(h_i)$.

Evaluation of the regional hurricane rate λ and the probability $P(h_i)$, the conditional probabilities $P(S_j \mid h_i)$, and the conditional probabilities $P(C > c \mid h_i, S_j)$ is the main objective of the hurricane model, the system model, and the consequence model, respectively. The probability $P(S_j \mid h_i)$ covers the states of the components of the HPS, such as closure structure and operations, precipitation levels, electric power availability, failures modes of levees and floodwalls, and pumping station reliability. To assess the state of the HPS given a hurricane event requires an evaluation of the reliability of individual structures, systems and components (e.g., levees, floodwalls, pump systems) when they are exposed to the loads and effects of the hurricane (e.g., the peak surge, wave action) and the relationship of these elements to the overall function of the system to prevent flooding in protected areas. A detailed description of the risk model is provided in Appendix 9.

Event Tree

The probability tree of Figure 4 was simplified to determine the rate of flooding levels and displaying the results as inundation contours within the basins. The processes of transforming inundation to consequences is simplified by grouping communication, warning decision and public execution into an *exposure factor* parameter applied to lives and property at risk, and grouping power and pumping availability into one event. The resulting event tree appropriately branched out is shown in Figure 6. The events of the tree are defined in Table 1.

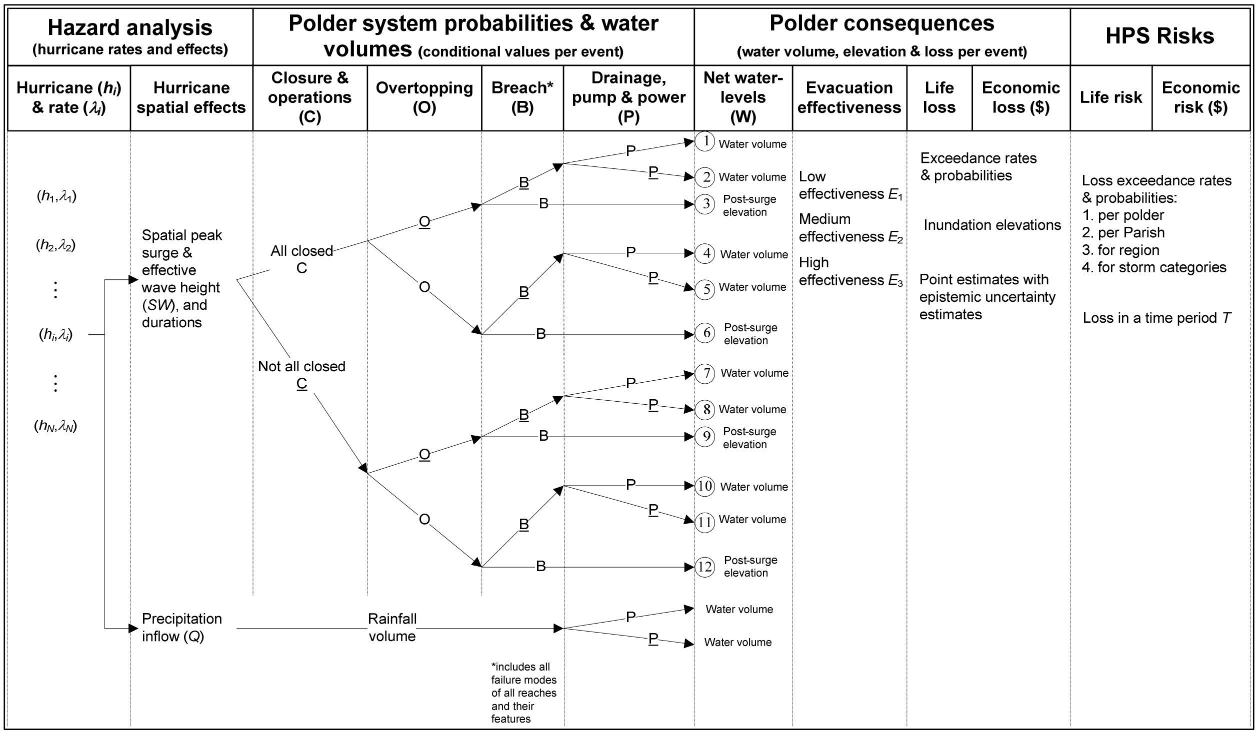

Figure 6. Event Tree for Quantifying Risk. Underlined events (i.e., C, P, O, and B) are the complements of the respective events (i.e., C, P, O, and B)

Table 1
Summary of the Event Tree Top Events

Top Event	Description
Hurricane initiating event	The hurricane initiating event is mapping of the peak flood surge with waves in the study area with a hurricane rate λ. This event was denoted, hi(x,y), and has a probability of occurrence, P(hi(x,y)) and a rate of occurrence of λP(hi(x,y)).
Closure structure and operations (C)	This event models whether the hurricane protection system closures, i.e., gates, have been sealed prior to the hurricane. This event depends on a number of factors as illustrated in the influence diagram. The closure structures are treated in groups in terms of probability of being closed in preparation for the arrival of a hurricane. This event was used to account for variations in local practices and effectiveness relating to closures and their operations.
Precipitation inflow (Q)	This event corresponds to the rainfall that occurs during a hurricane event. The precipitation inflow per subbasin is treated as a random variable.
Drainage, pumping and power (P)	This event models the availability of power (normal) power for the pump systems. This event is modeled in the event tree to represent a common mode of failure for the pump systems, and is included in developing a model for drainage and pumping efficiency or lack thereof including backflow through pumps. The event also models the availability of the pump system and its ability to handle a particular floodwater volume. This event is treated in aggregate with drainage effectiveness and power reliability including backflow through pumps.
Overtopping (O)	This event models the failure of the enclosure/protection system due to overtopping, given that failure has not occurred by some other (non-overtopping) failure mode. If failure (breach) does not occur, some flooding due to overtopping could result.
Breach (B)	This event models the failure of the enclosure/protection system (e.g., levees/floodwalls, closures) during the hurricane, exclusive of overtopping failures). This event includes all other failures and it models all ‘independent’ levee/floodwall sections. This event is treated using conditional probabilities as provided in Figure 6.

Risk Quantification

Functional Modeling and Computational Considerations. While the primary purpose of the HPS is to prevent water from entering protected areas during hurricanes, water may also enter the system during rainfall events and from groundwater. The protected areas of the HPS are sub-divided into basins and subbasins. This partitioning is based on the internal drainage and pumping system within each Basin. Figure 5 shows the New Orleans East basin and two sub-basins for illustration purposes. Basins and subbasins are divided into sections, or reaches, that have similar cross-sections, material strength parameters and foundation conditions.

The quantification of risk associated with the hurricane protection system requires the determination of the amount of water that is expected to reach the protected areas for a particular hurricane. The water entering the protected areas was determined to be the as a result of one or more of the following two cases:

1. non-breach events producing overtopping water volume, water volume entering through closures (i.e., gates) that are left open, precipitation, and potential backflow from pumping stations

2. breach events leading to water elevations in protected areas

The risk quantification framework was, therefore, based on obtaining estimates of water volumes and elevations entering the HPS due to one of these cases.

The event tree presented in Figure 6 shows the two quantities of interest in the net water levels column resulting from overtopping, precipitation, open closures, i.e., gates, and backflow from pumping stations in non-breach cases, and the post-surge elevation that would result in breaching cases. The branches of the rainfall volume are added to all the other branches for a particular hurricane. The figure shows a total of twelve branches that are constructed per hurricane. These sections describe the computations needed to quantify risk. They are presenting in a manner that correspond to the events shown in Figure 6, and were modeled in a spreadsheet to perform the computations. The sections that follow provide the background information and basis behind the approaches used for these computations.

Definition of Basins, Subbasins, Reaches and Features. The HPS is divided into basins, subbasins, reaches and features. Table 2 illustrates the information structure used to define selected reaches. The HPS definition includes the following basins:

1. Orleans West Bank (OW)
2. New Orleans East (NOE)
3. Orleans (OM)
4. St. Bernard (SB)
5. Jefferson East (JE)
6. Jefferson West (JW)
7. Plaquemines Area (PL)
8. St. Charles (ST)

Table 2
Definition of Reaches

Reach	Length (ft)	Elevation (ft)	Design Water Elevation (ft)	Reach Type	Reach Weir Coefficient	Polder Reference	Subpolder Reference
1	5.000E+03	4.000E+00	1.000E+00	L	2.6	NOE	NOE1
2	5.000E+03	4.000E+00	1.000E+00	W	3.0	NOE	NOE1
3	5.000E+03	4.000E+00	1.000E+00	L	2.6	NOE	NOE2
4	5.000E+03	4.000E+00	1.000E+00	W	3.0	NOE	NOE2
5	5.000E+03	4.000E+00	1.000E+00	L	2.6	NOE	NOE3
6	5.000E+03	4.000E+00	1.000E+00	W	3.0	NOE	NOE3
7	5.000E+03	4.000E+00	1.000E+00	L	2.6	NOE	NOE4
8	5.000E+03	4.000E+00	1.000E+00	W	3.0	NOE	NOE4
9	5.000E+03	4.000E+00	1.000E+00	L	2.6	NOE	NOE5
10	5.000E+03	4.000E+00	1.000E+00	W	3.0	NOE	NOE5

Table 3 illustrates the definitions of features within each reach for selected reaches. For each feature, the following information was developed:

- Feature number for unique identification
- Type of features of drainage structure (D), or closures (i.e., gate G), or transition structure (T)
- Reach in which the feature is located
- A reference value for correlated gates assigned the same probability of closure
- Length (ft) of water inflow when gates are left open
- Bottom elevation (ft) of gates
- Probability of not closing gates

Sources of Information – The Risk Team collected data from design documents, construction drawings and studies conducted by other IPET teams to develop detailed descriptions of the basins. Maps were assembled from aerial photos and information was overlayed in GIS files that included: lat/long data, geotechnical profiles and boring logs, crest elevations, stationing used to define reaches and the locations of critical features such as closure gates and pump stations. The information on these maps was confirmed by field surveys of the entire system by members of the risk team who traveled every mile of the system. Photos, GPS coordinates and notes were taken during these surveys to document each feature and reach used in the risk model. In addition to the maps, data was compiled for use in the reliability analyses and the risk model. This process has resulted in a comprehensive description of the HPS.

Reach Descriptions – The HPS perimeter is discretized into reaches that define sections that have similar physical and engineering characteristics. Initially the reaches were defined using the beginning and ending stations shown in the original design memoranda (DM). The stations were then adjusted based on examinations of the subsurface material information to form reaches that were expected to have similar performance (reliability). Basin descriptions are in Appendices 2 through 8.

Table 3
Definition of Features with Respective Reaches

Feature Number	Type	Reach	Correlated Features	Length (ft)	Bottom Elevation (ft)	Not-Closed Probability
1	G	1	1	5.000E+01	0	1.000E-01
2	G	1	1	5.000E+01	0	1.000E-01
3	G	2	3	6.667E+01	0	2.000E-02
4	G	2	3	6.667E+01	0	5.000E-01
5	G	2	3	6.667E+01	0	5.000E-01
6	D	1				
7	T	1				
8	G	3	8	1.250E+02	0	2.300E-01
10	D	3				
11	T	3				
12	G	7	12	1.500E+02	0	4.000E-02
13	D	7				
14	T	7				5.000E-03
15	G	14	15	7.500E+01	0	7.500E-02

Elevations of Crests – The elevations of the tops of walls and levees, adjusted to the current datum, of the entire New Orleans area HPS were developed for use in the suite of hurricane simulations and the risk assessment model calculations of water volumes from overtopping and breaching. Various sources elevations of segments of the HPS existed, some adjusted to current datum, but most were not. The 1 ft. and 15 ft. lidar on the IPET repository been adjusted to current datum and gave about a 99% coverage of the HPS system. These gave good values for portions of the HPS that had clear levees and numerous hard surveys were available for short portions of the walls, some of which been adjusted.

Using the 1 ft lidar where it was available, cross section profiles were cut approximately every 200-500 ft along the entire HPS. Where the 1 ft lidar was not available, the 15 ft lidar was used. For the levees, these elevations were compared to the current expected values obtained from various MVN records, Taskforce Guardian and any available hard survey information for verification. The location of walls, drainage structures, closures, and gaps were known from the sites visits and documented with photos and notes for the entire HPS. Some walls had adjusted hard survey info available but for most walls, it was necessary to go back to the lidar data and examine the areas by drawing numerous profiles, searching for patterns of “good hits” on wall tops and to determine the elevations of the surrounding soil. Then using the photos and notes obtained from the site visits, estimates of the wall elevations were made. This same process was used for transition regions. A final comparison to the elevations used in the ADCIRC grid developed by the Storm Team was made for consistency.

Hurricane Hazard Analysis. The hurricane hazard analysis method parameterizes hurricanes using their characteristics at landfall (central pressure drop, radius of maximum wind, etc.). From these values for historic events, the recurrence rate is estimated for hurricane events in a neighborhood of the region of interest the joint probability density function of the hurricane parameters in that neighborhood. The possible combinations of winds, surges and waves would be computationally demanding if every combination was run through the ADCIRC models. To reduce the number of runs a response surface approach was used. In this approach a relatively small number of hurricanes are selected and used to calculate the corresponding surge and wave levels at the sites of interest. Then a response surface model is fitted to each response variable (surge or wave level at a specific site). Finally, a refined discretization of parameter space is used with the response surface as a proxy model in place of the range of possible events to represent the hurricane hazard. The outcomes of these computations are combined surge and effective wave values at particular locations of interest along the hurricane protection system, e.g., representative values at the reaches. These values are denoted as h_i in Figure 6. A complete description of the method used to evaluate the hurricane hazard is presented in Appendix 8.

The water elevation required by risk model as a loading is taken as the surge elevation plus wave setup if waves are present. Surge only was not considered as a separate loading condition.

Hurricane rate modeling and prediction methods are then used to compute the corresponding exceedance rates to h_i values, and are denoted as λ_i in Figure 6. Also, the water elevation in a basin after a breach is termed the post-surge elevation. This post-surge elevation in a basin could be higher than the applicable lake or river water level.

The epistemic uncertainties in both the surge/wave elevation and the rates are considered as discussed separately in a subsequent section. Figure 7 illustrates surge water elevation as a function of time, i.e., hydrographs, at stations defining the hurricane protection system for one storm. The hurricane rates were also obtained and used to construct a peak elevation exceedance curve for a station as illustrated in Figure 8. Details of the actual hydrographs are provided in Appendix 8. Table 4 illustrates information and results related to hurricane simulations that include:

- Hurricane run numeric identification
- Hurricane rates
- National Hurricane Center Category designation
- Reach overtopping volume mean and standard deviation with computational models provided in subsequent sections

Overtopping Flow Rate and Volume Models, and Probabilities

Deterministic Models. The overtopping volume was computed using the rectangular weir formulae (Daugherty et al. 1985) for a given water elevation and length of reach for each hurricane

Uncertainty Analysis. The uncertainty in the water volume calculations uses Monte Carlo simulation and nonlinear curve fitting based on least squares to propagate uncertainty in the weir equation. The uncertainty analysis of the overtopping flow rate was assessed using Monte Carlo simulation based on a normally distributed epistemic uncertainty of the water height at a reach for a particular hurricane run.

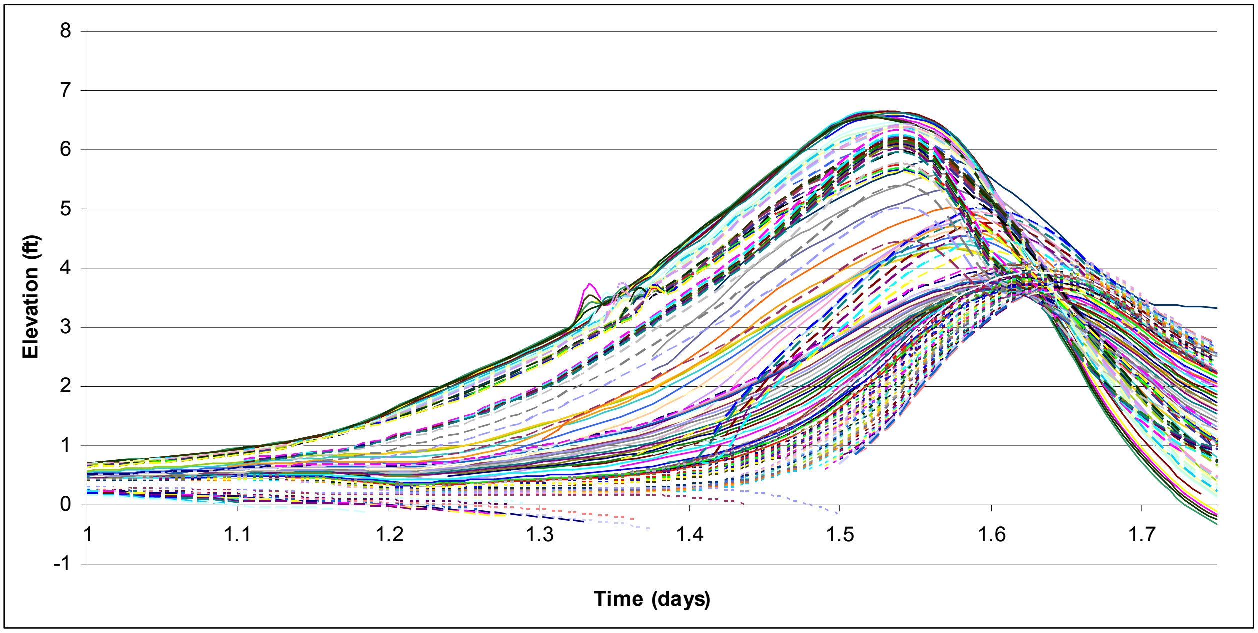

Figure 7. Hydrographs at Stations Defining the Hurricane Protection System for a Storm

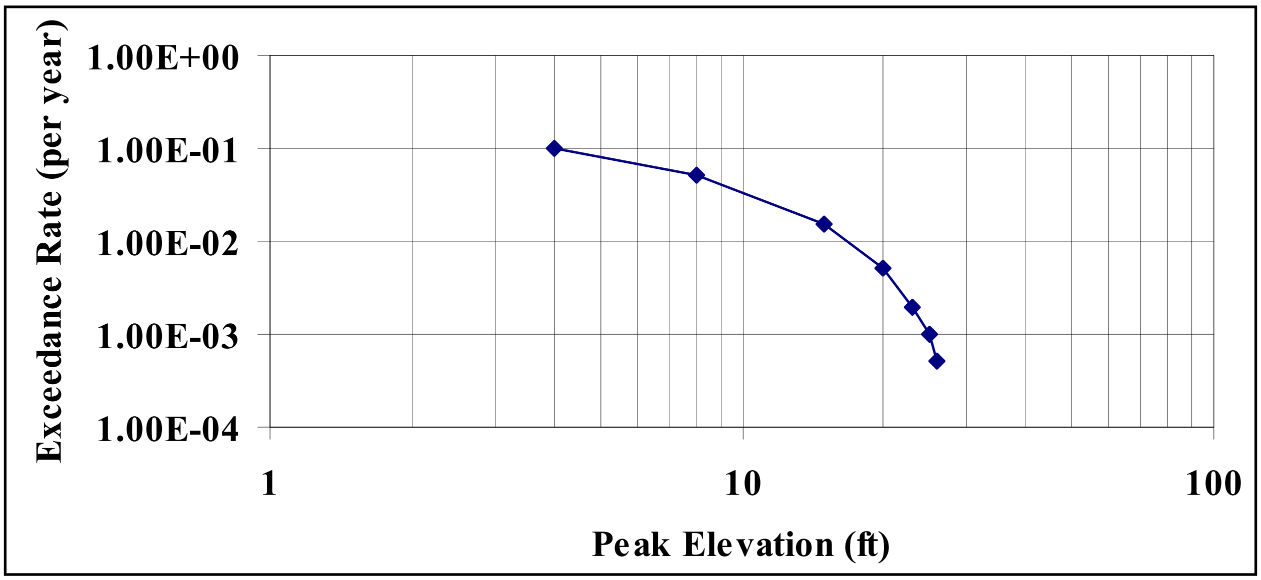

Figure 8. Surge and wave Exceedance Curve Corresponding to a Station

Table 4
Hurricane Runs, Rates, Category, and Reach Overtopping Volume Results

Run	Rate (Events/Yr)	Category	OW1-M Mean (ft^3)	OW1-S StD (ft^3)	OW2-M Mean (ft^3)	OW2-S StD (ft^3)	NOE1-M Mean (ft^3)	NOE1-S StD (ft^3)
1	1.000E-01	I	0.000E+00	0.000E+00	0.000E+00	0.000E+00	8.276E+03	1.655E+03
2	5.000E-02	III	0.000E+00	0.000E+00	0.000E+00	0.000E+00	1.655E+04	3.310E+03
3	1.000E-02	IV	0.000E+00	0.000E+00	0.000E+00	0.000E+00	3.310E+04	6.621E+03
4	7.500E-02	III	0.000E+00	0.000E+00	0.000E+00	0.000E+00	1.655E+04	3.310E+03
5	2.000E-02	II	0.000E+00	0.000E+00	0.000E+00	0.000E+00	3.310E+04	6.621E+03
6	2.000E-01	I	0.000E+00	0.000E+00	0.000E+00	0.000E+00	8.276E+03	1.655E+03
7	5.000E-03	IV	0.000E+00	0.000E+00	0.000E+00	0.000E+00	3.310E+04	6.621E+03
8	9.000E-02	II	0.000E+00	0.000E+00	0.000E+00	0.000E+00	1.655E+04	3.310E+03
9	1.500E-01	I	0.000E+00	0.000E+00	0.000E+00	0.000E+00	8.276E+03	1.655E+03

Failure and Overtopping Probability. Failure probabilities including overtopping probability was computed based on a performance function as commonly used in structural reliability assessment (see for example Ayyub 2003; Ayyub and McCuen 2003) as given by

$$Z = R - L \tag{3}$$

Where Z = performance function, R = strength (resistance) and L = loading in the structure. In this case the resistance is provided by the hurricane protection elevation, and the loading is provided by the surge/wave elevation. The non-performance probability was computed as

$$P = \text{Prob}\ (g < 0) \tag{4}$$

Once the total volume was obtained from all overtopping and breach cases, the net volume (as a random variable) needed for consequence analysis was computed by adding water volume from rainfall, and the effect of pumping that includes backflow. The pumping volume and backflow are considered as a multiplier called the pumping factor.

Illustrations. Table 4 provides typical results for a reach. Several hypothetical reaches were used to construct overtopping results that were aggregated by subbasins as illustrated in Table 5. In this example, the basin is assumed to contain one or more subbasins. The overtopping results for this subbasin include the overtopping volume based on an overtopping condition and the overtopping probability was computed using system reliability concept.

Water Volumes from Other Features of the Protection System. The hurricane protection system includes other features that could allow water volume to enter the protected areas during a hurricane. These features include:

1. closure structures, i.e., gates, that are left open or failed to close
2. localized changes in levee or floodwall elevations that create a transition in the HPS

These features are identified within each reach and assigned to subbasins in case of non-performance. For the closure structures case, the water volume resulting from failure of the closure structure for a given hurricane was computed based on respective gate closing failure probabilities, width of the closure structure and elevation of the bottom of the structure. The water volume associated with the localized changes in levee or floodwall elevations requires identification of the changes in elevation and the lengths over which the elevation varies. Table 5 shows a tabulated structure for computing volumes associated with features.

Table 5
A Tabulated Structure for Water Volumes for Subbasins and Basins

Subpolder Number	Overtopping Volume (V|OT)		Precipitation Rainfall Volume		Closures Water Volume		Breach Volume Elevation		Breach Volume Volume	
	Mean (ft^3)	StD (ft^3)	Mean (ft^3)	StD (ft^3)	Mean (ft^3)	StD (ft^3)	Mean (ft)	StD (ft)	Mean (ft^3)	StD (ft^3)
OW1	0.000E+00	0.000E+00	0.000E+00	0.000E+00	0.000E+00	0.000E+00	1.187E+00	5.937E-02	1.743E+08	4.571E+06
OW2	0.000E+00	0.000E+00	0.000E+00	0.000E+00	0.000E+00	0.000E+00	1.187E+00	5.937E-02	4.858E+08	9.056E+06
NOE1	0.000E+00	0.000E+00	1.655E+04	3.310E+03	4.724E+02	7.162E+01	1.187E+00	5.937E-02	4.461E+08	3.157E+07
NOE2	0.000E+00	0.000E+00	3.775E+06	7.551E+05	4.977E+02	9.954E+01	1.187E+00	5.937E-02	1.109E+09	1.355E+07
NOE3	0.000E+00	0.000E+00	2.703E+06	5.406E+05	0.000E+00	0.000E+00	1.187E+00	5.937E-02	3.059E+08	5.171E+06
NOE4	0.000E+00	0.000E+00	1.550E+01	3.100E+00	5.972E+02	1.194E+02	1.187E+00	5.937E-02	8.688E+07	2.631E+06
NOE5	0.000E+00	0.000E+00	9.367E+07	1.873E+07	0.000E+00	0.000E+00	1.187E+00	5.937E-02	2.463E+09	2.281E+07
OM1	0.000E+00	0.000E+00	0.000E+00	0.000E+00	0.000E+00	0.000E+00	1.187E+00	5.937E-02	7.075E+08	9.807E+06
OM2	0.000E+00	0.000E+00	0.000E+00	0.000E+00	0.000E+00	0.000E+00	1.187E+00	5.937E-02	6.399E+08	8.787E+06
OM3	0.000E+00	0.000E+00	0.000E+00	0.000E+00	0.000E+00	0.000E+00	1.187E+00	5.937E-02	2.480E+08	6.962E+06
OM4	0.000E+00	0.000E+00	0.000E+00	0.000E+00	0.000E+00	0.000E+00	1.187E+00	5.937E-02	7.016E+07	2.248E+06
OM5	0.000E+00	0.000E+00	0.000E+00	0.000E+00	0.000E+00	0.000E+00	1.187E+00	5.937E-02	4.371E+08	1.257E+07
SB1	0.000E+00	0.000E+00	0.000E+00	0.000E+00	0.000E+00	0.000E+00	1.187E+00	5.937E-02	1.753E+08	5.671E+06
SB2	0.000E+00	0.000E+00	0.000E+00	0.000E+00	0.000E+00	0.000E+00	1.187E+00	5.937E-02	1.367E+06	4.737E+04
SB3	0.000E+00	0.000E+00	0.000E+00	0.000E+00	0.000E+00	0.000E+00	1.187E+00	5.937E-02	1.491E+08	4.839E+06
SB4	0.000E+00	0.000E+00	0.000E+00	0.000E+00	0.000E+00	0.000E+00	1.187E+00	5.937E-02	1.581E+07	2.990E+06

Breach Elevation and Volume Models.

Three Cases of Breach Failure Within Reaches. The risk quantification was effectively performed by examining three cases of breach failure that correspond to branches presented in the event tree of Figure 6. The three cases are:

1. breach given overtopping
2. breach given no overtopping
3. breach due to feature (closure gate, pump house, etc.) failures

The first case of breach given overtopping is primarily driven by erosion resulting from overtopping water flow. Fragility curves for these cases were developed as described in the reliability methodology Appendix 10

Breach Parameters. The inundation mapping of the risk analysis was based on determining the volume of water entering a basin due to levee/floodwall overtopping and/or breaching, open gates and rainfall. The breaching scenarios require knowledge of the breach size, depth and surge hydrograph at the breach in order to determine basin inflows. The Katrina experience was reviewed to identify basic characteristics of the major breaches in order to develop general rules to use in the risk model for breach size.

One critical characteristic that determines the volume of water flowing through a breach is the duration of time that the breach is open. Katrina proved that the breaches could not be repaired in time to have an effect on the level of water achieved inside the basins. Therefore the duration that the breach is open was assumed to have no effect on inflow volumes and water elevations.

IPET studies indicate that the Katrina induced London Ave. and 17^{th} St. canal breaches occurred before the water level in the canals reached the top of wall and appear to have been the result of a foundation or design failure. Therefore, this would be a breach given no overtopping scenario in the risk analysis. The high water marks (HWM) experienced during Katrina inside the Orleans basin where the canal breaches occurred and the length of time that surge elevations exceeded lake levels in the canals were examined. Experienced HWM during Katrina in the basins were very close (within about 1') to the peak surges in the canals. For example, it appears that the London Avenue South breach occurred when the canal water level was at about 7 to 8 feet, or 3' or so below the top of wall. The peak surge in the area was about 10-11 feet and HWM is also about 10'. The hydrographs experienced in those areas show that the time that the surge elevation exceeded the failure elevation was on the order of several hours. It appears that this was sufficient time for the water elevations inside the basin to closely follow the surge levels. The inverts of the canal breaches were at or below the normal lake level so water flowed back into the lake after the surge passed. Based on this it would seem appropriate to use the peak surge level as the water elevation achieved inside the basin when a catastrophic breach (full levee height) occurs during a non-overtopping event.

Therefore for a breach that occurs without overtopping, the following assumptions are used in the risk model:

- All breaches would be considered to be a result of a structural or foundation failure and would be catastrophic (full depth of levee or floodwall).
- The breach depth would extend to or below lake or river level.
- The maximum interior water levels caused by the breach would be the same as the maximum surge level experienced adjacent to the breach.

For the case of a breach during an overtopping event, a reliability model for overtopping erosion was development. The erosion model for levees is expected to show different breach inverts based on the amount of overtopping from surge or waves and the type of soil in the levee. In the case where the breach invert is higher than lake or river level, the depth and length of the breach, the duration of time that the surge exceeds the breach invert and the weir coefficient through the breach is required to calculate inflow volumes. The breach widths for the levees and floodwalls could also be expected to be similar to that experienced during Katrina. Breach widths at the major canal breaches varied (450 to 1000+ feet) but were all on the order of several hundred feet. At the industrial canal (IHNC) where overtopping did occur, the two Lower Ninth Ward breaches were similar in width to the other canals where overtopping did not occur, and the depth of the breaches were below the normal canal water levels so water also flowed back through these breaches when the surge passed. Based on these observations, using the peak surge level as the maximum water elevation achieved inside the basin would be appropriate when a catastrophic breach (full levee height) occurs during an overtopping event.

For the case of a less than catastrophic breach given overtopping, it was necessary to calculate the basin inflow volume over the reach from overtopping in the same manner as for the non-breaching case and add an amount that would account for the flow through the breach. The risk model does not consider breaches that are less than catastrophic. The risk model considers the mean depth of overtopping required to cause a full breach and estimates the uncertainty in that value. This method provides a conservative estimate of basin inflows by assuming the breach width, depth and weir coefficient and then calculating the inflow volume in the same way that the open-gate inflow volume is calculated. Some suggested overtopping values are shown in the table below.

Therefore for a breach that occurs during an overtopping event, the following assumptions are used in the risk model:

- Breaches would be as a result of an erosion failure due to surge and/or waves.
- All breach depths are assumed to be full levee height however the depth of overtopping required to cause a breach is dependent upon soil properties. Assumed values are shown in the table below.

Levee/Wall Material	Overtopping Depth (ft) for Full Breach	
	Mean	Std Dev
Clay	6'	2'
Sand/Clay	4'	2'
Hydraulic Fill	2'	2'

- Durations of overtopping are based on the surge hydrographs.
- The interior water levels in the basin would be the same as the surge level for the Full depth levee breach.

Basin Reliability Analysis. Failure modes, performance functions, basic random variables, and computational procedures of failure probabilities used in the fragility analyses are provided in Appendix 10.

Water Elevation and Volume. The surge hydrograph produced by a hurricane is used to compute the water volume entering a basin during levee overtopping or breaching, and the maximum water elevation within the Basin. In the case of levee overtopping, the water elevation within a basin is based on a water volume computed and the duration of overtopping. If a breach occurs and the invert of the breach is below the final elevation of the adjacent body of water, the water elevation is the elevation of that body of water. If the breach invert is above the final elevation of the adjacent body of water, the water elevation is based on a water volume entering the basin computed using the duration that the surge is above the breach invert. The topography of the Basin, and the drainage and pumping models were used to construct this relationship. An example of this relationship was provided in the 2000 unwatering plan of the greater metropolitan area of New Orleans, LA prepared by the District in 2000 which has figures that relate stage elevation to storage. Figure 9 shows such a stage-storage plot for the New Orleans East (Citrus).

An example of one of these relationships is shown for New Orleans East Basin Figure 10 for the subbasins shown in Figure 1. For the purposes of the risk model, rather than using fitted curves, stage-storage relationship were numerically evaluated and tabulated in increments of 1 ft of elevation and linear interpolation was used.

The computations of water elevations in subbasins after allowing for interflow among the subbasins at the connections, i.e., interfaces, was complicated when a basin has two or more subbasins in which flooding is controlled by separate pumping and drainage systems. The cases of two to five subbasins are discussed herein. For the two subbasin case, the computations of the final volumes were used as a basic case to iteratively determine water volumes and elevations for the cases of more than two subbasins. Appendix 9 provides the procedures used in the interflow analyses.

Figure 9. Stage-Storage Relationship of New Orleans (Citrus)

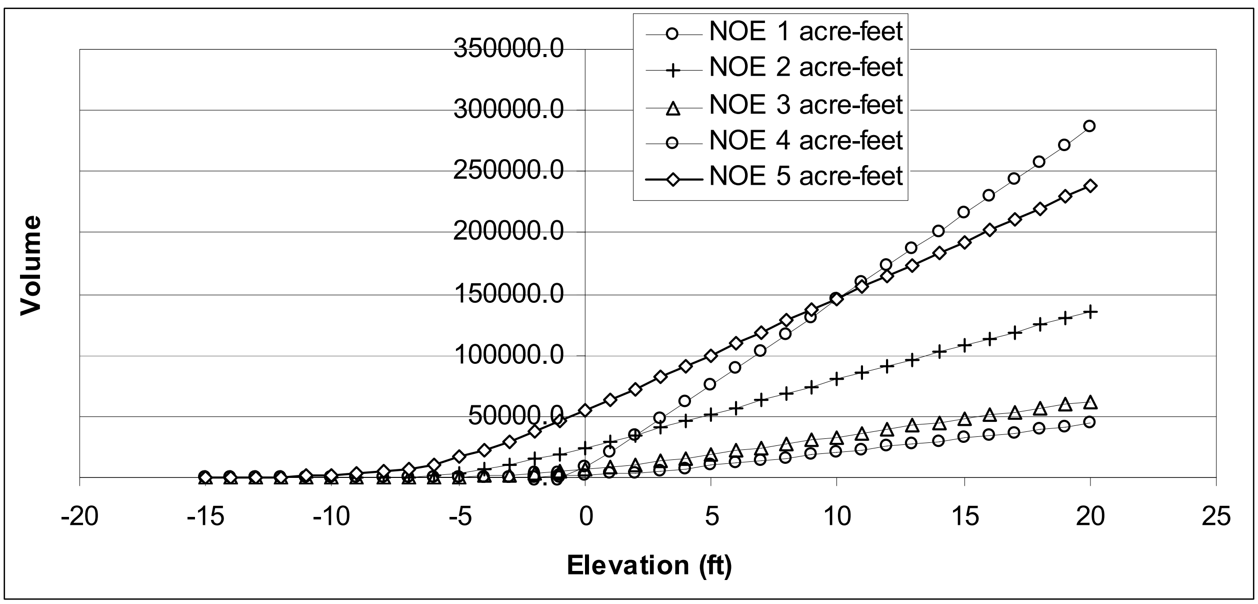

Figure 10. Stage-Storage Relationships of Subbasins and Basin New Orleans East

Event Tree Branch Probabilities. The event tree of Figure 6 consists of 12 branches per hurricane. Appendix 9 provides the details of the process used to develop these probabilities for these branches.

The event tree includes the following primary independent subbasin-level events:

- The event that *all gates* within a subbasin are closed

- The event that *all pumps* in the subbasin work
- The event that at least one reach (or one of its features) in a subbasin is breached

Risk Profile by Water Elevation. The results produced were summarized by subbasin, and for all storms and the branches of the event tree in the form of water elevation (mean and variance) and occurrence rates. These results were used to evaluate elevation-exceedance rate for a subbasin at selected water depths.

Monetary and Life Loss Risk Profiles. Monetary and life losses were estimated and results were provided as elevation-loss curves per subbasins by the Consequence Team. Figure 11 provides example results for selected subbasins. Using results from elevation-loss curves per subbasin, loss-exceedance as shown in Figure 11 were developed.

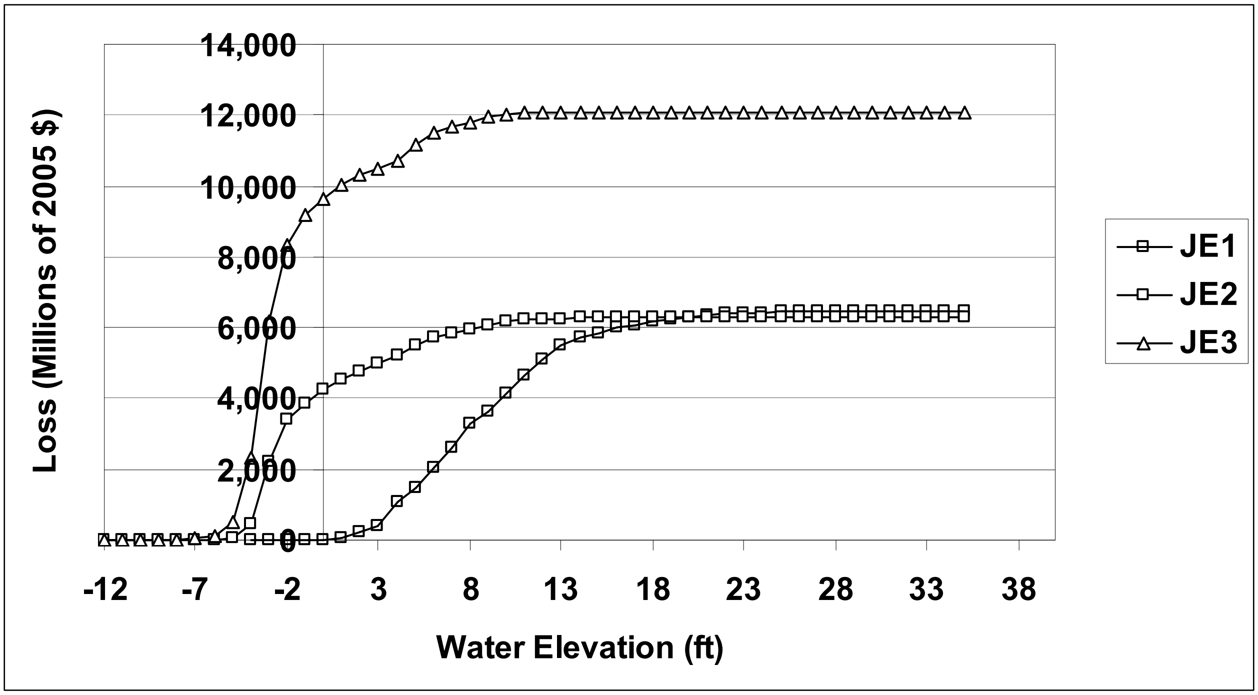

Figure 11. Elevation-Loss Curves for Jefferson East (JE) Subbasins

Risk Profile by Basins and Storm Categories. The risk profiles for basins and storm categories were evaluated by performing the corresponding aggregation similar to what is done for the subbasins, and results displayed using curves similar to those provided in Figure 12. The risk profile for the HPS is only be expressed in terms of the direct economic and life loss consequences based upon the stage-damage curves provided by the Consequences Team. This risk profile requires that all storms be evaluated for all possible combinations of all the branches for all the basins with dependency modeling. The number of combination per storm for 8 basins and 10 branches of the event tree is 1,073,741,824. Dependency among the basins has not been examined in order to reduce the number of possible combinations, however the risk results obtained by examining the individual basins is considered to be adequate for evaluating the relative risks and vulnerabilities in the HPS.

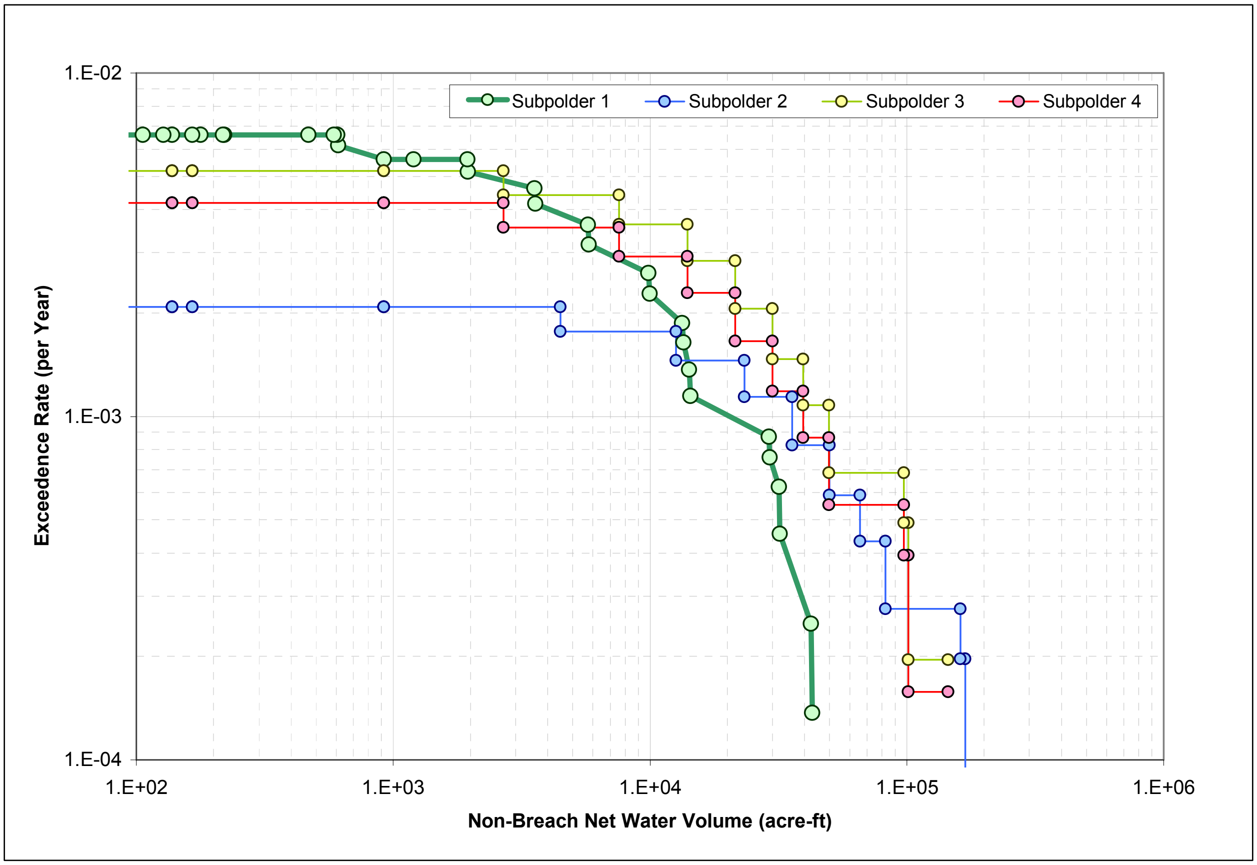

Figure 12. Overtopping Risk Profile for Subbasin

Hazard Analysis and Initiating Events

The initiating events selected for study in the risk analysis of the HPS was based upon the range of hurricanes considered to be possible in the New Orleans area that would be capable of causing widespread damage and flooding. The Risk Team relied upon the basic analysis techniques and procedures used by the Storm Team to conduct the hindcast of the Katrina event, however the approaches were modified to account for the large number of storms that were required to be studied in a probabilistic hazard analysis. Several methods have been used in other studies to quantify hurricane hazard, typically in the context of wind-related risk. The methods available to conduct probabilistic hurricane surge and wave predictions in the context of a risk analysis is limited. These methods are generally classified into three main types: historic (HI), joint-probability (JP), and Monte Carlo simulation (MC) methods. Details of the hazard analyses is provided in Appendix 8.

Historic Methods

Historic methods quantify the hazard based on the rate at which the effect of interest, (e.g., wind speed or surge or loss) has occurred in the historical record. These methods are fundamentally nonparametric, i.e. they do not assume a specific analytic form for the recurrence rate of the hurricanes or their effects. One problem with purely nonparametric historic approaches is the "granularity" of the results that reflects the small number of significant events in the historical record and the sensitivity of the results to unusual occurrences ("outliers") during the observation period. To reduce these effects, some historic approaches include smoothing procedures. For example, the empirical simulation technique (EST) of Sheffner et al. (1996) "smears" the influential historical hurricanes by replacing them with a suite of hypothetical events with somewhat different characteristics, typically with different landfall locations. Other smoothing methods fit a specific distribution to the hurricane effects L_i calculated from the historic events. An example of the latter type is the 1987 version of the National Hurricane Center Risk Analysis Program HURISK (Neumann 1987). The EST method has been extensively used by the USACE and FEMA to identify design events with return periods, up to 100 years. Confidence intervals on the results are usually obtained through bootstrapping (resampling) techniques.

Joint Probability (JP) Methods

Joint probability methods make a parametric representation of hurricanes, typically based on their characteristics at landfall and the filling rate after landfall. For hurricanes these characteristics include the location and velocity vector, the central pressure deficit, the radius to maximum winds and the track followed by the hurricane prior to landfall. The historic record is used to estimate the recurrence rate. The effects of interest are then calculated for a representative set of the characteristic values and, by combining these values with the estimated recurrence rate, the recurrence rate of the parameter set is obtained.

Monte Carlo Simulation Methods

Monte Carlo simulation methods use a stochastic representation of the origin and temporal evolution of hurricanes in the general region of interest, in this case the North Atlantic region. The random trajectory and parameter evolution are typically represented through Markov processes of suitable order, discrete in time but continuous in state. The state-transition parameters vary spatially and are estimated from the historical record. A large number of hurricane events are simulated using this random dynamic model. The sample is trimmed to retain only the events that are considered to be significant to the region and the effects of interest and the retained events are treated like the historical sample in the HI methods. As in the joint probability method, when the number of retained events is too large to evaluate the responses with high accuracy, it is necessary to use parsimonious high-accuracy runs in combination with less accurate methods. The MC simulation method was first proposed by Vickery et al. (2000). More recent studies that use MC simulation are Huang et al. (2001) and Powell et al. (2005).

Choice of a Method

The attractiveness of a method depends in general on the amount of data and computational resources available as well as the objective of the analysis. Regarding the latter, it matters whether (1) interest is in frequent or rare events, (2) the objective is to identify design events with given return periods (return-period analysis) or find the rate at which certain consequences are exceeded (risk analysis), and (3), in the case risk analysis, whether the losses occur in a small geographical region that may be considered uniformly impacted by any given hurricane or over an extended region where spatial homogeneity of the hurricane loads cannot be assumed. For flood hazard, return-period analysis is generally easier than risk analysis because hurricane severity may be ranked using surrogate quantities (such as a rough estimate of maximum surge) that are much easier to calculate than the flooding conditions themselves.

Since medium to long return periods are of interest, historical methods are discarded. Both JP and MC methods can handle such return periods. Monte Carlo approaches face the problem of sorting out the potentially damaging events from large suites of simulated hurricane scenarios. This is not a trivial problem for the geographically extended and differently vulnerable system we are considering. For these reasons, the joint probability approach has been selected. This approach is further described in the following sections.

To implement a joint probability method for hurricane hazard, it is convenient to describe hurricanes at landfall through the following parameters

- ΔP (mb) = central pressure deficit at landfall
- R_{max} (km) = radius to maximum winds at landfall
- X (km) = longitudinal landfall location relative to downtown New Orleans (positive if east of New Orleans)
- θ (degrees) = direction of storm motion at landfall, ($\theta = 0$ for tracks pointing north, increasing clockwise)
- V (m/s) = storm translation speed at landfall
- B = Holland's radial pressure profile parameter at landfall (Holland 1980)

While the variation of these parameters before and after landfall is also of interest, the primary characterization of hurricanes required in the risk studies is in terms of their properties at landfall. Hence the main tasks of the hazard quantification for the initiating events in the risk analysis is the estimation of the hurricane recurrence rate and the evaluation of the wave and surge loads over a suitable range of characteristic parameters.

Hurricane Recurrence at Landfall

Information used to estimate recurrence rates includes historical data sets (mainly NOAA's HURDAT data for frequency, ΔP, X, θ and V and data on R_{max} from Ho et al. 1987) as well as published distribution results. The HURDAT data set (Jarvinen et al. 1984, and recent updates) has been used to extract values of (ΔP, X, θ, V) at landfall over the stretch of coastline between longitudes 85W and 95W. For recurrence analysis, only storms of hurricane strength at landfall have been considered (defined as those having measured or estimated $\Delta P \geq 25$ mb) since 1890. Earlier events have been neglected because prior to 1890 the historical record is incomplete and less accurate. The HURDAT data set has been used also to analyze pre-landfall conditions.

Information on the structure and parameterization of hurricanes provided in various references, including Holland (1980), Ho et al. (1987), Vickery and Twisdale (1995a,b), Chouinard et al. (1997), Vickery et al. (2000), Huang et al. (2001), Willoughby and Rahn (2004), and Powell et al. (2005). For the coastal area of interest here, the main findings of these studies are:

The distribution of ΔP may be assumed to be either lognormal or Weibull. The Weibull distribution tends to give better fits to the data when all tropical storms are included, whereas the lognormal model is more appropriate when only hurricanes are considered; see Vickery and Twisdale (1995a). Using the lognormal model and a locally weighted maximum-likelihood procedure, Chouinard et al. (1997) found that along the Louisiana Coast the standard deviation of ΔP is almost constant at 21 mb, whereas the mean value of ΔP increases eastward from about 32 mb near the Texas border to about 38 mb near the Mississippi border. This trend is attributed to the sea temperature anomaly of the Loop Current.

Depending on coastal location, the distribution of θ is generally found to be normal or a mixture of two normal distributions, one for easterly storms and the other for westerly storms (Vickery and Twisdale 1995a; Huang et al. 2001).

Vickery et al. (2000) found that V may be taken to be lognormally distributed, with mean value about 6 m/s and standard deviation about 2.5 m/s. V has a mild dependence on θ, increasing as θ increases (Vickery and Twisdale 1995a).

$R_{\max}$ decreases with increasing hurricane pressure deficit ΔP and its conditional distribution given ΔP may be taken to be lognormal (Vickery and Twisdale 1995a; Powell et al. 2005). Using data from Ho et al. (1987), Vickery et al. (2000) fitted several linear and quadratic models to $\ln R_{\max}$ against ΔP and latitude. Willoughby and Rahn (2004) obtained qualitatively similar results when regressing $\ln R_{\max}$ against latitude and maximum wind speed.

B varies with $R_{\max}$ and possibly ΔP or maximum wind speed $V_{\max}$ and latitude (Holland 1980, Vickery et al. 2000, Willoughby and Rahn 2004, Powell et al. 2005). For storms of hurricane strength, Vickery et al. fitted several relations using data from different flight height ranges. Willoughby and Rahn (2004) studied the dependence of B on $R_{\max}$, $V_{\max}$, and latitude, finding that the distribution of B is nearly symmetrical and somewhat flatter and shorter-tailed than a normal distribution. Although Willoughby and Rahn estimate a linear dependence of B on $ln\, R_{\max}$, the slope coefficient is only marginally significant. The data analyzed by Powell et al. (2005) is a subset of that of Willoughby and Rahn. The Powell et al. subset uses selection criteria (high winds, low-level flights, and geographical location) that are relevant also to the present study.

The above observations have been used in the modeling of hurricane characteristics. However, dependencies, distribution types and parameter values have been sometimes modified based on further data analyses. Two data sets are used: a broad longitude (BL) data set, which includes HURDAT data at landfall for all hurricanes at ($\Delta P \geq 25$ mb) since 1890 that made landfall between longitudes 85W and 95W. The narrow longitude (NL) data set is the subset with landfall locations between 87.5W and 92.5W. Appendix 8 provides details of the process used to select the

Pre- and Post-Landfall Parameter Variation

The parameterization concerns exclusively the hurricane characteristics at landfall. One possibility, which has often been used in hurricane hazard analysis, is to assume straight paths and constant values of ΔP, $R_{\max}$, V and B prior to landfall; see for example Russell (1971), Batts et al. (1980), Georgiou et al. (1983), Neumann (1991), and Vickery and Twisdale (1995a). A more refined approach is used for the hurricane path and the pre-landfall variability of these parameters, as described in the following sections.

Pre-Landfall Parameter Variation. All tropical storms (not just hurricanes) after 1890 in the HURDAT record that made landfall within latitudes 85W and 95W are used to estimate the mean hurricane path for landfall angles θ around $-60^{\circ}, -30^{\circ}, 0, 30^{\circ}, 60^{\circ}$. Results are shown in Figure 13, where the dots represent average locations at 12 hour intervals relative to the time of landfall. These paths are used in all the hurricane analyses.

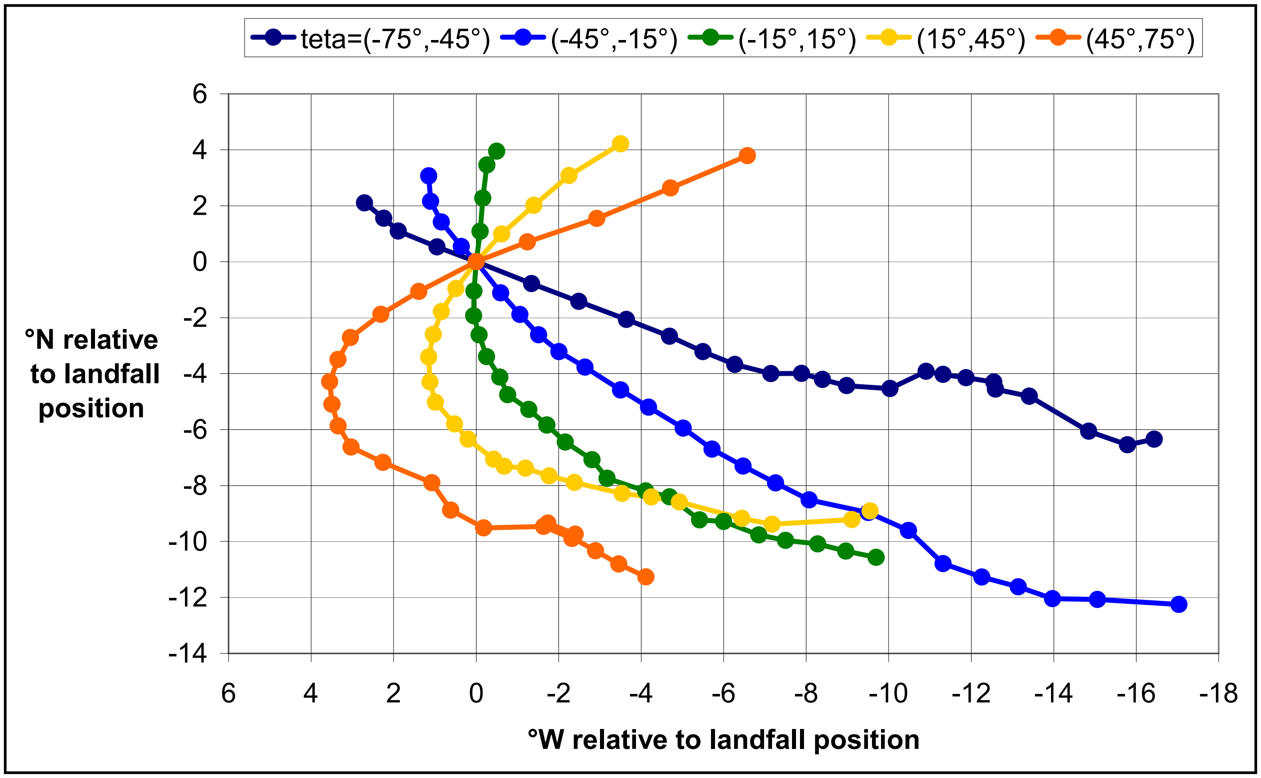

Figure 13. Mean Hurricane Path Depending on Landfall Angle θ

Post-landfall Conditions. After landfall, several hurricane parameters undergo significant changes. For example, the pressure deficit ΔP decreases in an approximately exponential way and the radius of maximum winds $R_{\max}$ tends to increase. The only change that may have significant effect on surges and waves is the temporal decay of ΔP.

Parameter Discretization for Risk Analysis

Hurricane risk is evaluated by considering a large number of possible scenario hurricanes, each associated with one set of storm characteristics. These scenario events are selected considering the joint probability method of analysis.

The possible range of hurricane characteristics in the New Orleans area define a region in parameter space. A possible discretization of this region is given by all combinations of the parameter values listed in Table 6

The parameters above the dashed line in Table 6 refer to conditions at landfall and those below the dashed line are for conditions before or after landfall. The first three values of ΔP in Table 6 are representative of hurricane Categories 2, 3 and 4 whereas the last three values represent various levels within Category 5.

Not all of the 26,250 possible hurricane scenarios in Table 6 need be considered for risk assessment: some may be excluded because they are exceedingly rare and others because they are unlikely to cause significant losses. For example, hurricanes with small $R_{\max}$ and large $|X|$ do not pose a threat to the New Orleans region. Also, depending on the sensitivity of the loads L to each parameter, the number of parameter levels may be reduced. Conversely, if a better representation of a parameter or a more accurate decomposition of risk is required, then the number of levels may be increased. This is especially true for ΔP.

Table 6
Parameter Levels that May be Considered for Risk Analysis

Parameter	Levels for risk analysis
ΔP (mb)	41, 59, 80, 100, 115, 130
V (km/h)	8, 15, 21, 27, 36
$X\cos(\theta)$ (km)	-130, -90, -50, -10, 30, 70, 110
θ	-60, -30, 0, 30, 60
$R_{\max}$	10%, 50%, 90% quantiles from Eq. 8-2
B	5%, 25%, 50%, 75%, 95% quantiles from Eq. 8-3
————————	--
$\Delta P_R(t)$	smooth $\Delta P_{R,0.5}(t)$ curve in Figure 8-5
$V_R(t)$	smooth $V_{R,0.5}(t)$ curves in Figure 8-6 depending on V
$R_{\max}(t)$	from $R_{\max}$, $\Delta P(t)$ and $Lat(t)$; see Eq. 8-5
$B(t)$	from B, $R_{\max}$ and $Lat(t)$; see Eq. 8-6
α	0.035 + 0.0005 ΔP
No. of cases	**26,250**

Assessment of Hurricane Loads

Finding the environmental loads for each parameter set of interest is the most challenging task of hurricane hazard characterization. The following paragraphs describe how this is done for still water levels, waves, and rainfall intensity.

Still Water Levels and Waves. It is well known that surge and waves interact (surge affects waves and vice-versa). Therefore, these loads should be ideally assessed using a coupled formulation. Sophisticated coupled programs are currently being developed that reflect this coupling, but at the present time such programs are not at a stage that they can be routinely used.

An alternative is to follow an iterative approach, whereby the surge H(x,y,t) without waves are first calculated, the wave field estimated given the preliminary estimate of the surge, and finally the surge code is re-run considering the calculated wave field. While the treatment of waves for the risk analysis uses a simple wave parameterization scheme based on results obtained in previous detailed analyses. This parameterization approach should produce rather accurate results and greatly streamlines computations (Robert Dean, personal communication). Surges are calculated using the ADCIRC code (Luettich et al. 1992).

ADCIRC uses a triangular grid with spatially varying resolution, which for the risk analysis application covers the entire Gulf of Mexico. The resolution increases in coastal areas, in particular near the Louisiana Coast. High-resolution grids may include millions of nodes and must be run with time steps on the order of 1 second to avoid numerical problems. Such dense grids produce accurate results and can adequately resolve topographic effects on horizontal scales of tens of meters along the coast.

Since it is not feasible to use such dense computational grids for all the parameter combinations in Table 6, a different strategy was adopted to avoid, running all cases by using computational grids at lower resolutions.

Reduction in the Number of ADCIRC Runs. Two conditions were taken advantage of reduce the number of runs: (1) If the dependence of the results on a parameter A is smooth, then results were calculated for a subset of levels of A and interpolation used for the other levels, and (2) If two parameters A and B do not interact (additively or multiplicatively), then the (additive or multiplicative) effect of varying one of them is the same irrespective of the level of the other parameter. In this case all combinations of A and B was inferred by varying each parameter while keeping the other parameter constant. Determination of whether either condition applies was made using a low-resolution (LR) ADCIRC grid run with only a few thousand nodes ignoring the effect of waves.

These considerations reduce the number of needed ADCIRC runs from about 26,000 in Table 6 to about 1,000. However, even 1,000 hurricane scenarios are too many to be run with a high-density grid. The strategy selected is to run these cases with a medium-resolution (MR) grid with approximately 90,000 nodes and use the high-resolution (HR) grid for only about 40 cases. The HR runs are then used to calibrate the MR results.

The spatial pattern of surge and waves depends primarily on R_{max}, X *and* θ. Since the effect of these parameters at a given geographic location is generally non-monotonic, interpolation involving these parameters would not produce accurate results. In addition, these parameters interact among themselves. Hence, all combinations of R_{max}, X *and* θ in Table 6 must be run using the MR model. The use of only 3 levels of R_{max} in Table 6 reduces the computational effort in the MR runs.

The LR runs have shown that, for given R_{max}, X *and* θ, the water level at each geographical location depends smoothly on ΔP, *V,* and *B*. Therefore a smaller number of levels of these parameters were considered and water levels calculated for the other levels through interpolation. This has led to the MR run plan in Table 7.

One may reduce the number of MR runs even further. From the LR runs, it was determined that the multiplicative effect of Holland's *B* on the surge depends mildly on ΔP and *V*. Therefore there is no need to run different values of *B* with each combination of ΔP and *V*. This produces the MR plan in Table 8, which comprises two sub-factorials of the levels in Table 7, with a total of only 1155 runs.

Table 7
Parameter Levels for Mid-Resolution Runs

Parameter	Levels for mid-resolution analysis
ΔP (mb)	41, 80, 115
V (km/h)	8, 21, 36
$X cos(\theta)$ (km)	-130, -90, -50, -10, 30, 70, 110
θ	-60, -30, 0, 30, 60
R_{max}	10%, 50%, 90% quantiles from Eq. 8-2
B	5%, 50%, 95% quantiles from Eq. 8-3
---------------	--
$\Delta P_R(t)$	smooth $\Delta P_{R,0.5}(t)$ curve in Figure 8-5
$V_R(t)$	smooth $V_{R,0.5}(t)$ curves in Figure 8-6 depending on V
$R_{max}(t)$	from R_{max}, $\Delta P(t)$ and $Lat(t)$; see Eq. 8-5
$B(t)$	from B, R_{max} and $Lat(t)$; see Eq. 8-6
α	$0.035 + 0.0005\,\Delta P$
No. of cases	**2835**

Table 8 Final Plan for the Mid-Resolution Runs		
	Mid-resolution model runs	
Parameter	**Factorial 1**	**Factorial 2**
ΔP (mb)	41, 80, 115	80
V (km/h)	8, 21, 36	21
$Xcos(\theta)$ (km)	-130, -90, -50, -10, 30, 70, 110	-130, -90, -50, -10, 30, 70, 110
θ	-60, -30, 0, 30, 60	-60, -30, 0, 30, 60
R_{max}	10%, 50%, 90% quantile from Eq. 8-2	10%, 50%, 90% quantile from Eq. 8-2
B	50% quantile from Eq. 8-3	5%, 95% quantiles from Eq. 8-3
---------------	--	--
$\Delta P_R(t)$	$\Delta P_{R,0.5}(t)$ from Figure 8-5	$\Delta P_{R,0.5}(t)$ from Figure 8-5
$V_R(t)$	$V_{R,0.5}(t)$ from Figure 8-6	$V_{R,0.5}(t)$ from Figure 8-6
$R_{max}(t)$	from Eq. 8-5	from Eq. 8-5
$B(t)$	from Eq. 8-6	from Eq. 8-6
α	0.035 + 0.0005 ΔP	0.035 + 0.0005 ΔP
No. of runs	**945**	**210**
Total runs	**1155**	

For the HR runs, the subset of 36 hurricanes in Table 9 is retained. In general, the levels in Table 9 have been chosen to maximize the accuracy of calibration of the MR results. The individual hurricane paths considered in the risk analysis are shown in Figure 14.

Table 9 Factorial Plan for the High-Resolution Runs	
Parameter	**High-resolution model runs**
ΔP (mb)	80, 115
V (km/h)	21
$Xcos(\theta)$ (km)	-90, -10, 70
θ	-60, 0, 60
R_{max}	10%, 90% quantiles from Eq. 8-2
B	50% quantile from Eq. 8-3
-----------------	---
$\Delta P_R(t)$	$\Delta P_{R,0.5}(t)$ from Figure 8-5
$V_R(t)$	$V_{R,0.5}(t)$ from Figure 8-6
$R_{max}(t)$	from R_{max}, $\Delta P(t)$ and $Lat(t)$; see Eq. 8-5
$B(t)$	from B, R_{max} and $Lat(t)$; see Eq. 8-6
α	0.035 + 0.0005 ΔP
No. of cases	**36**

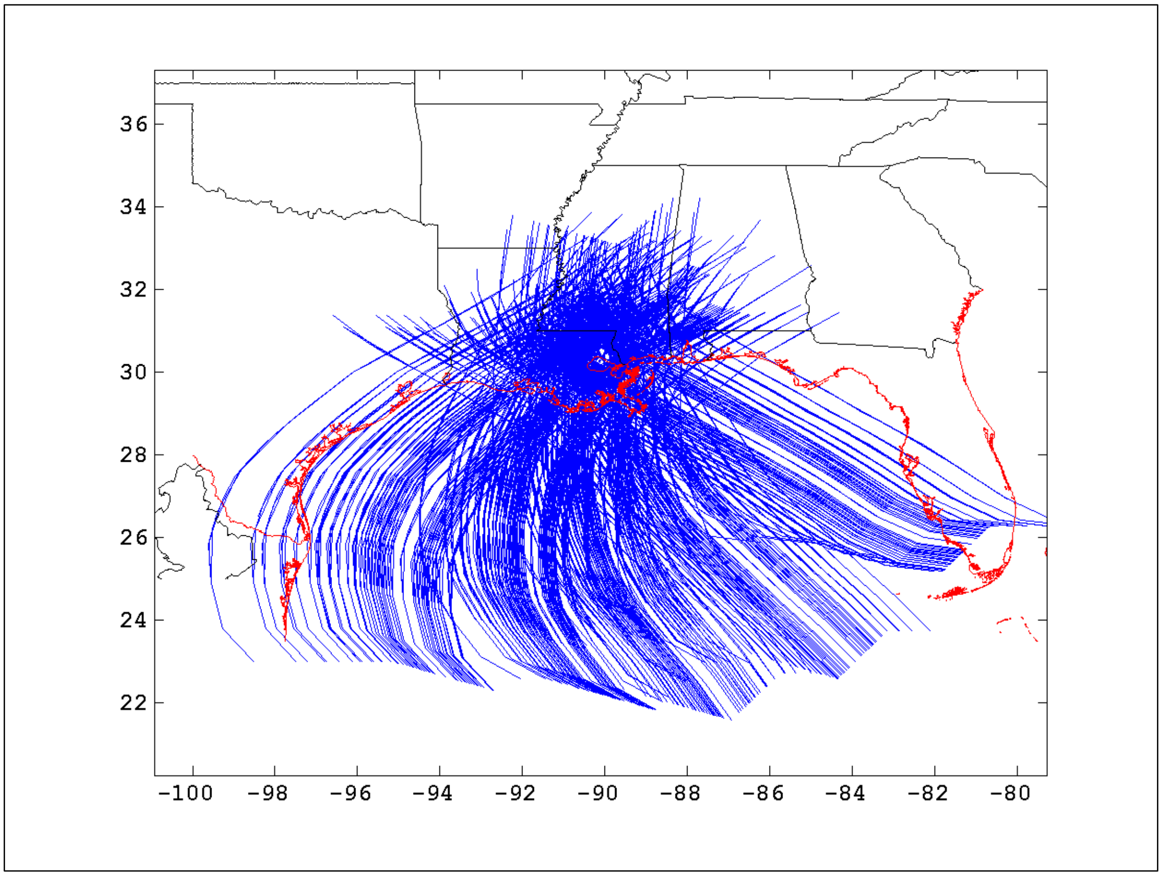

Figure 14. The Individual Hurricane Paths Considered in the Risk Analysis

Calibration and Extension of the MR Results Using the HR Runs

For the high resolution subset of the MR runs (the HR runs) the final water levels are taken directly from the simulations. However, for the remainder of the MR cases, it was necessary to make corrections to adjust for a relative lack of resolution of the MR grid. These corrections are site-specific, depending on the local geometry of the coast, the topography, and the different local land coverage of the MR and HR grids. The correction further depended on the hurricane parameters; in particular, the correction at a given location will generally depend on landfall position X, direction θ, and possibly storm intensity ΔP and radius to maximum winds, R_{max}.

The calibration procedure applies to locations at which the MR grid produces realistic results. At locations where this is not so, for example along narrow canals where the MR values are not reliable or may not exist (because the MR grid does not extend to those locations), a different strategy was used. For this case, HR results were used to fit regression relations in terms of values along the coast where the MR solution is available. Then fitted regressions were used to extrapolate the estimates from preceding corrections. The calibration process is described in detail in Appendix 8.

Rainfall Intensity

Rainfall is among the variables that affect the inundation of the basins. While rainfall is not of primary concern for the hurricane protection system, it is a contributor to the frequency of low-level flood losses. Hence it was decided that a relatively coarse model of hurricane-induced rainfall would suffice.

Prior to NASA's Tropical Rainfall Measuring Mission (TRMM) (Simpson et al. 1988), information on hurricane rainfall was scanty. The TRMM mission, which started in November 1997, produced vast amounts of rainfall estimates for tropical storms and hurricanes at a spatial scale of about 5 km in various tropical regions, including the Atlantic basin. These rainfall products have been analyzed statistically by Lonfat et al. (2004) and Chen et al. (2006). The model used is based primarily on these two studies and on discussions with Dr. Shuyi Chen at the University of Miami. The model is described in detail in Appendix 8.

Assessment of Rainfall Intensity Inside the Basins. A simplified model of rainfall inside the basins was developed as described in Appendix 8. First the mean rainfall contribution from the symmetric component of the mean rain field was selected. Next the asymmetric component and finally the variability of rainfall around the mean were assessed.

For hurricanes that pass to the right or near the basin, the azimuthal dependence of the rainfall field is conservatively neglected. For hurricanes that pass to the left of a basin, the asymmetric component is accounted for by multiplying the above symmetric mean rainfall values by 1.5. This factor includes intensification due to land effects.

Uncertainty is expressed by a lognormal random variable with mean value 1 and log standard deviation 0.69, which corresponds to an uncertainty factor of 2. This random factor is applied to the entire mean rainfall time history. In reality, rainfall intensity inside a basin would display significant fluctuations in time and space, which locally could far exceed a factor of 2. However, the above random factor is considered adequate to reflect uncertainty on the total precipitation in a basin during the passage of a hurricane.

Epistemic Uncertainty

Epistemic uncertainty (uncertainty due to limited information and knowledge) affects all aspects of the hazard characterization. While a thorough assessment of these uncertainties is beyond the scope of this project, a rough quantification of uncertainty on the hurricane rates and the loads was made.

General Considerations. The hurricane rates are uncertain due to the limited historical sample size, possible errors in the assumed form of marginal and conditional distributions (especially in the tail regions), and the uncertain near-future hurricane activity due to fluctuations and trends associated with climate changes and multi-decadal cycles. A first-order assessment of uncertainty on hurricane rates is based on the hurricane effects of global warming and shorter-term climatic fluctuations in the North Atlantic.

Causes of epistemic uncertainty on wave and surge levels are hurricane model errors, for example the wind field idealization, the coefficient of friction with the water surface, the effects of waves on water level, etc., are estimated by hind casting historical events or by comparing results from different modeling assumptions.

Climatic Effects and Their Contribution to Epistemic Uncertainty

The potential effect of global warming on the frequency, size and intensity of tropical cyclones is a hotly debated issue in the technical literature; see Pielke et al. (2005), Emanuel (2005b), and Elsner (2005) for recent reviews. Theoretical analysis, numerical modeling and historical data analysis have all been used to study the effects of climate variations on various features of tropical cyclones. The main results on hurricane frequency and intensity are summarized below. What determines hurricane size is poorly understood; hence the possible dependence of $R_{\max}$ on global warming and other climatic factors is not considered.

Frequency of Tropical Cyclones. The frequency of tropical cyclones worldwide has remained remarkably constant during the past 100 years or more (Elsner and Kocher 2000; Webster et al. 2005; Emanuel 2005b). Since during this period the planet has undergone global warming and cooling, it is concluded that climatic changes of this type and magnitude have small effects on the rate of tropical cyclones at the planetary scale.

On the other hand, significant fluctuations in tropical cyclone activity at decadal and multi-decadal scales have occurred in various parts of the world. For example, hurricane activity in the North Atlantic was low in the 1970s, 1980s, and early 1990s compared with the 1940s, 1950s and early 1960s or with the decade since 1995. Changes in hurricane frequency between active and quiescent periods have been by factors of 2 or more (Goldenberg et al. 2001). The current rate in the North Atlantic is about 50% higher than the historical average rate and will likely persist at least over the next 5 years (Elsner 2005). These fluctuations are due to well-known cycles like the El-Nino-Southern Oscillation (ENSO), which by increasing the wind shear dampens the rate and intensity of hurricanes, the tropical Atlantic sea-surface temperature (SST), with warmer temperatures usually producing higher hurricane rates, and the Atlantic multi-decadal oscillation (AMO), which is the difference in air pressure between Iceland and the Azores and is thought to affect mainly the hurricane tracks (Elsner 2005).

Intensity of Tropical Cyclones. The effect of global warming on tropical cyclone intensity is somewhat more controversial. It has been argued that an increase in sea surface temperature would make the atmosphere more thermodynamically unstable and increase the maximum potential intensity (PI) of hurricanes (Emanuel 1987; Lighthill et al. 1994; Henderson-Sellers et al. 1998). In turn, PI has been shown to be highly correlated with the average intensity of hurricanes (Emanuel 2000). Following this argument, increases in intensity under a warmer climate may be expected (Emanuel 2005a). It may also be argued that an increase in sea surface temperature would increase the vertical wind shear, which tends to disrupt the symmetry of tropical cyclones and reduces their intensity.

Empirical evidence of higher hurricane intensity during the past 50 years, when the sea surface temperature has increased by about 0.2 degree centigrade, is weak (Landsea et al. 1999;

Bister and Emanuel 2002; Free et al. 2004; Chan and Liu 2004). This is in agreement with findings based on global circulation models. For example, Knutson and Tuleya (2004) and Michaels et al. (2005) predict increases in wind speed of 5% or less by the year 2080. Therefore, while future variations in intensity due to global warming are considered possible, it is generally expected that such variations was modest and overshadowed by the multi-decadal fluctuations.

Results that contrast with this general consensus are reported in Emanuel (2005a). Using data worldwide, Emanuel found that the energy released by hurricanes has increased by about 70% over the past 30 years and attributes the phenomenon to global warming. This phenomenon is contributed by an increase of 15% in the maximum wind speed and an increase of 60% in storm duration. These findings have been contested by other researchers and must be considered preliminary pending further validation.

Epistemic Uncertainty on Future Hurricane Climate. From the preceding discussion, uncertainty on the hurricane statistics in the Gulf of Mexico during the next 50-100 years is dominated by multi-decadal oscillations. Specifically, considering that the North Atlantic is now experiencing a 50% higher-than normal activity and that this elevated activity may persist over a number of years and possibly decades, it is reasonable for the next 50-100 years to increase the average historical rate of hurricanes by 20% and allow for an additional 25% uncertainty factor around this corrected rate. The latter factor includes uncertainty on the historical rate due to the finite observation period (16%) as well as uncertainty on the future evolution of the hurricane frequency (judgmentally assessed).

Considering the general consensus and dissenting views on the effect of global warming on hurricane intensity, the historical mean pressure deficit is increased by 3% and an uncertainty factor of 5% is applied to the increased mean value. Since the effects of different factors on hurricane frequency and intensity are poorly correlated, these components of epistemic uncertainty may be treated as independent.

Hurricane Waves

Introduction. An approximate method has been used for calculating waves and wave setup due to hurricane winds over the Gulf of Mexico. The quantification of deep water waves is based on a method published in the Shore Protection Manual[1] (1984). The wave setup is based on the physics governing wave setup, considers an average slope over the profile and employs the Dally et al (1985) wave breaking relationship over the full range from deep to shallow water. The method is described in detail in Appendix 8.

The Shore Protection Manual (SPM) provided recommendations for calculating deep water wave characteristics in a hurricane. These methods included two equations, one for the maximum significant wave height and one for the associated wave period. In addition a graph was provided which represented the non-dimensional distribution of wave heights in a hurricane.

[1] The predecessor to the Coastal Engineering Manual of the U.S. Army Corps of Engineers.

Setup on Levees. Levee conditions are considered in two classes: (1) Non-overtopped, and (2) Overtopped. Recommendations are presented below for each class.

Non-overtopped Levees. A definition sketch of a non-overtopped levee is shown in Figure 15. The water depth including storm surge on the seaward side of the levee is denoted h_1. The recommended total wave setup is the wave setup η_1 that has occurred due to waves propagating to the depth h_1 and the additional wave setup on the levee, η_2, i.e., $\eta_T = \eta_1 + \eta_2$. The wave setup at the depth, h_1 is determined with the use of Figure 16 which shows the percentage of the total setup which occurs seaward of a particular relative water depth. It is seen that most of the wave setup occurs in water depths relatively near to the breaking depth. This is a consequence of the Dally, et al breaking model on a very mild slope. This is the wave setup at the toe of the levee and should be added to the water depth which includes wind surge, etc.

Summary. The methodology used to model waves is necessarily approximate due to the time and resources available, but does represent a first step toward the goal of accounting for wave setup, a real process in storm surge. Mechanisms not accounted for here include the effects of vegetation and bottom friction which are known to reduce wave setup.

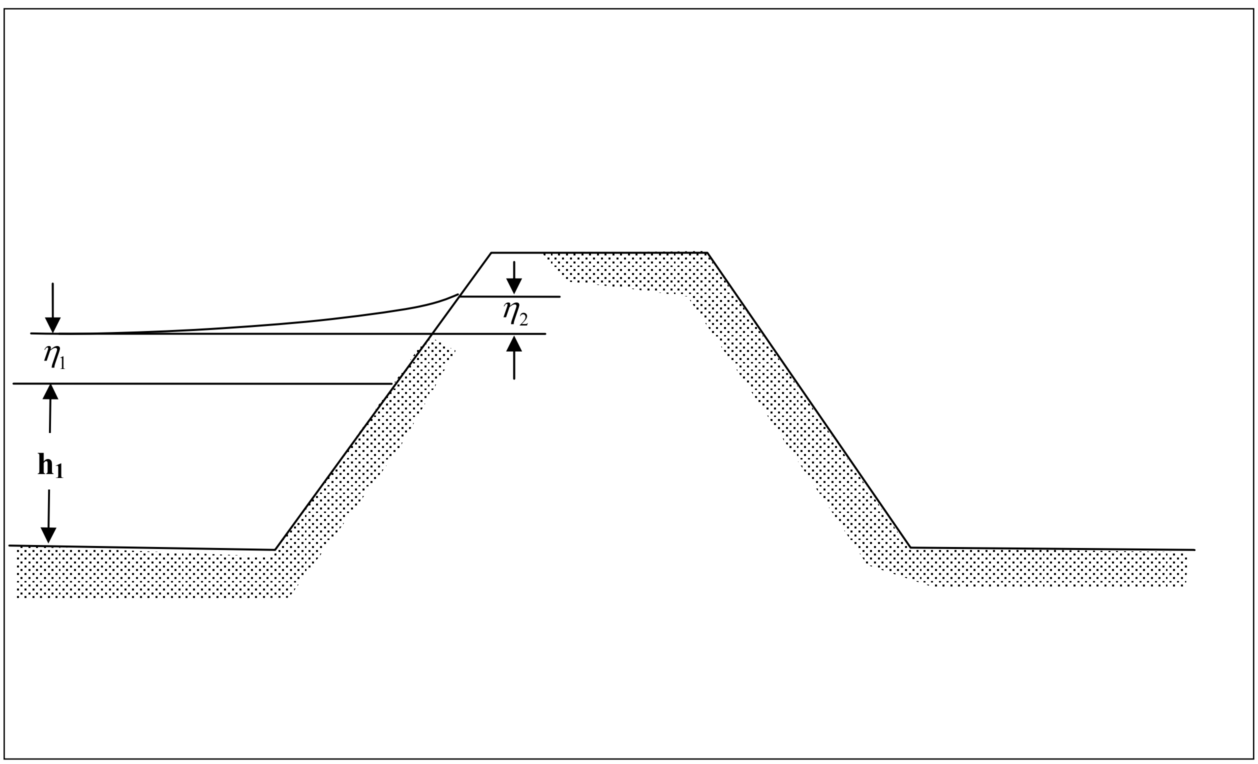

Figure 15. Definition Sketch for Non-Overtopped Levee

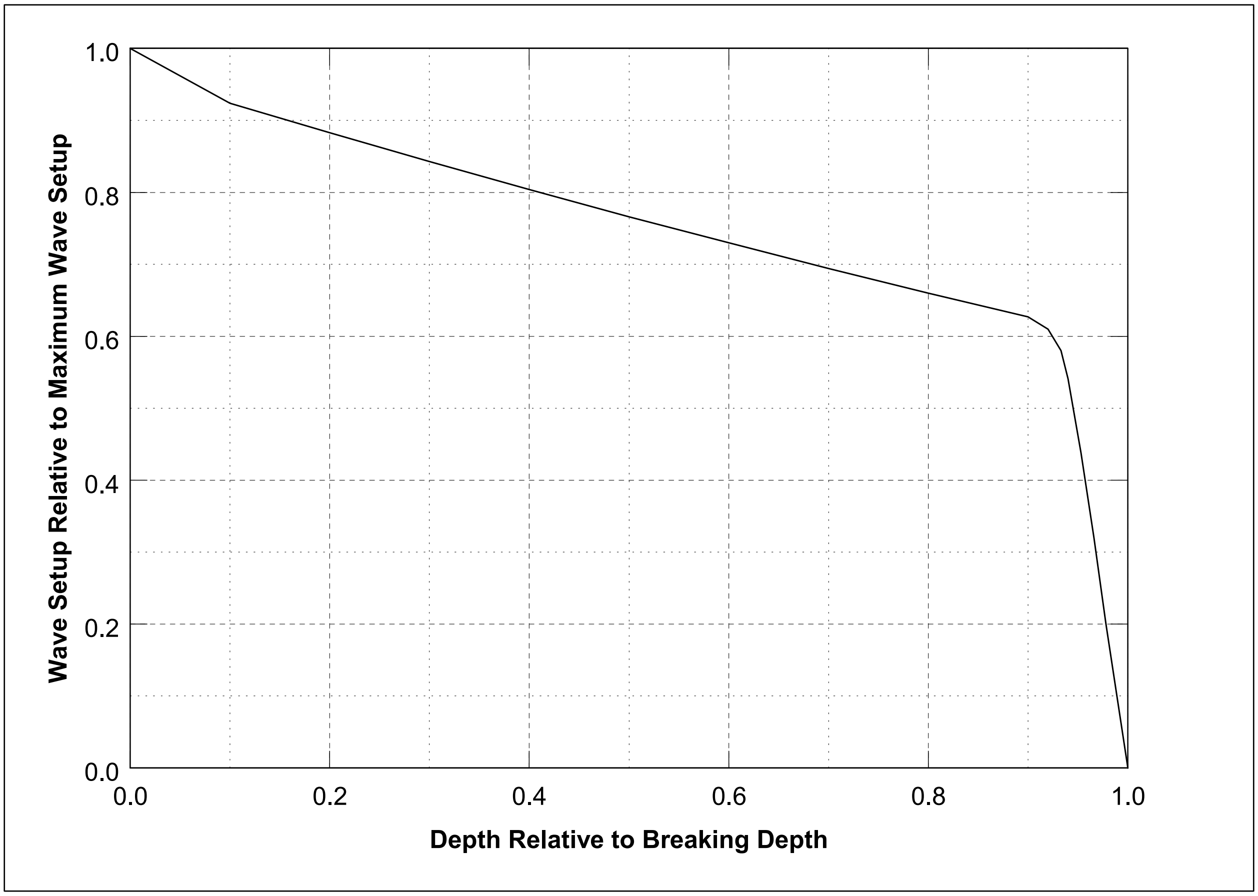

Figure 16. Proportion of Maximum Wave Setup that has Occurred versus a Proportion of the Breaking Depth

Determination of Hurricane Frequencies

Each storm considered in the MR1 ADCIRC simulation set is envisioned to represent all possible storms with similar values of radius, central pressure, and so forth. Accordingly, a rate of occurrence is assigned to each storm, representing the total rate of occurrence of all similar storms.

The controlling factors are the overall density of storms in space and time – λ_0 – and the fractional occurrence rates of each of a storm's several defining parameters. These are the central pressure deficit, ΔP, the radius to maximum winds, R_{max}, the forward translation speed of the storm, V, the shoreline crossing angle, θ, and the crossing location, X. The fractional occurrence rates for the parameters are derived from the cumulative probability distribution functions for each, by dividing the CDF into segments centered on each selected parameter value.

For example, crossing angles of -60, -30, 0, 30, and 60 degrees clockwise from north were selected for simulation. The fraction of all storms represented by the discrete value 30, say, is equal to the total probability mass for all angles between 15 and 45 degrees. This is simply the difference between the angle-CDF values at 15 and 45 degrees. This is the approach used for angle, forward speed, radius, and central pressure, although some adjustment of the pressure probabilities are needed, as discussed in Appendix 8. The radius to maximum winds is handled in a different manner. Examples of storm frequencies are also shown in Appendix 8.

Reliability Analysis

Reliability analysis is that part of the risk study that leads to an evaluation of the conditional probability of failure (i.e., reliability) of structures, systems, and components when they are exposed to the loads of a hurricane. The reliability analysis had three steps:

1. Specify the structures, components, and systems constituting the hurricane protection system (HPS) for each drainage basin.
2. Define *failure* and identify failure modes and limit states for each structure, system and component.
3. Assign conditional probabilities to HPS failure states for given water elevations caused by hurricane conditions.

Two conditions were analyzed for the reliability of levees, flood walls, and pumping stations: pre-Katrina and post-reconstruction and repair as projected for June 2006.

Appendices 2 through 7 contain an inventory of the structures, systems, and components in each drainage basin that were considered in the risk analysis. Subsystems and components of the HPS are shown in Table 10. The reliability methodology is described in detail in Appendix 10.

Table 10
Components in the Hurricane Protection System

1	Levees	a. Embankment section (Reaches were defined on the basis of physical discontinuities - geometric, physical, soils, and construction characteristics) b. Foundation
2	Floodwalls	a. Wall structure b. Joints within a wall section c. Transitions (joints and interfaces to other components) d. Wall-embankment interface e. Wall foundation
3	Closures	a. Closure support structure b. Closure structures - logs, gate, or other c. Position – open or closed
4	Pump Systems	a. Pump and motors b. Power – grid availability c. Emergency power (diesel generator) d. Diesel fuel availability e. Pump house structure f. Operators – present or evacuated g. Intakes – open or closed

Approach

The reliability of the hurricane protection system under potential water elevations due to surge and waves was quantified using structural and geotechnical reliability models integrated within a larger system description of each drainage basin. The reliability models for the HPS components were developed based on design and construction information, and on the results of the Performance Team and the Pump Stations Team studies. Reliability models were developed and evaluated to determine dominant, or most likely, failure modes for each reach defined in a drainage basin.

The reliability models included uncertainties in structural material properties, geotechnical engineering properties, subsurface soil profile conditions, and engineering performance models of levees, floodwalls, and transition points. Uncertainties due to spatial and temporal variation, and due to limited knowledge are tracked separately in the analysis, providing a best estimate of the frequency of failure under given loads, along with a measure of the uncertainty in that frequency.

The HPS was comprised of levees, flood walls, levees with floodwalls on top, and various points of transition or localized facilities such as pumping stations, drainage works, pipes penetrating the HPS, and gates. Each drainage basin perimeter was divided into segments, referred to as reaches, which were deemed to be homogeneous in three respects: structural cross-section, elevations in the cross section, and geotechnical cross-section. For example, 30 such reaches were identified for the New Orleans East (NOE) drainage basin.

Geometric and engineering material properties were identified for each reach and summarized in data tables. Structural cross-sections were initially identified by review of as-built drawings, aerial photographs, and GIS overlays; and were subsequently confirmed in on-site reconnaissance. Elevations were assessed in the same reconnaissance, supplemented by LIDAR and field surveys provided to the Risk Team. Geotechnical cross-sections and corresponding soil engineering properties were derived from original USACE General Design Memoranda (GDM) for the respective project areas of each drainage basin, supplemented by site characterization data collected post-Katrina at levee and flood wall failure sites (cone penetrometer and laboratory measurements on undisturbed samples).

Engineering performance models and calculations were adapted from the GDM's. Engineering parameter and model uncertainties were propagated through those calculations to obtain approximate fragility curves as a function of water height for components of the HPS. These results were calibrated against the analyses of the Performance Team, which applied more sophisticated analysis techniques to similar structural and geotechnical profiles in the vicinity of failures. Failure modes identified by the Performance Team were incorporated into the reliability analyses as those results became available.

Reliability assessments were performed for individual reaches of the HPS for given water elevations. This resulted in fragility curves for each reach by mode of failure. A fragility curve gives the probability of failure, conditional upon an event (water elevation in this study), at which a limiting failure state is exceeded.

Reliability assessments for each reach and component of the drainage basin perimeter were combined in the HPS risk model. The risk model used the water elevations from the hurricane hazard and the HPS fragilities to calculate probability of volume and duration of flooding within each drainage basin. The system risk model is structured around an event-tree description of the occurrence of hurricane events, corresponding water and wave heights, and the resulting response of the HPS. The risk model separately tracks natural variations and knowledge uncertainties from both the hurricane hazard and the structural and geotechnical response, to give a best estimate of frequency and duration of flooding, along with measures of uncertainty in those frequencies.

Definition of failure

Failures that lead to breach of the drainage basin perimeters were associated with four principal failure modes: (1) levee or levee foundation failure, (2) floodwall or floodwall foundation failure, (3) levee or floodwall erosion caused by overtopping, and (4) failure modes associated with point features such as transitions, junctions, and closures. The Performance Team found no failures in the HPS which originated in structural failure of the I-wall or T-wall components. All documented failures at I-wall and T-wall locations were geotechnical in nature, with structural damage resulting from the geotechnical failures.

Each reach within the drainage basin perimeter was analyzed and tracked separately, so that the number of failed reaches and their location around the drainage basin perimeter was known for each repetition of the HPS risk model.

The pumping system may have a mitigating effect on the water elevation of each drainage basin. If the capacity of the pumping system is exceeded by the inflow volume from a single breach then the number and location of the breaches may not matter and the pumping system can be ignored in the risk analysis. If, however, the inflow volume is within the capacity of the pumping system to remove, then the probability that the pumps are operating must also be calculated.[2]

The Risk Team has relied on other IPET Teams to clarify technical issues. Technical input from other Teams helped the Risk Team determine the level of detail with which failure states need to be represented.

Hurricane Protection System

The HPS for each drainage basin has four components: (1) levees, (2) I-walls (which may be atop levees), (3) T-walls (which may be atop levees), and (4) transitions and closures. The reliability analysis examined the performance of the each of component, separately and in combination.

The following structures in the HPS were not independently evaluated for their failure modes: (1) concrete aprons associated with some I-walls, and (2) sheetpiles with a short (3 to 4 ft.) concrete cap. Either could be addressed with failure modes developed for I-walls, but were not included in the present study.

The following failure modes or contributing factors were not considered in the reliability analysis:

[2] Data for evaluating the effect of pump station operation on basin water elevations was not available for the HPS risk analysis.

1. Internal erosion (piping) of levees due to seepage; note, this is in contrast to high pore pressures in sand strata, which was considered, as in the vicinity of the London Avenue Canal or the northern end of the IHNC. Internal erosion may be reconsidered in later studies.
2. The effects of maintenance on the HPS capacity over time. Improper maintenance or neglect can lead to reduced capacity of the levees in particular; gates and other moving components also require maintenance. Trees, landscaping, and pools were observed on protected embankments after Hurricane Katrina, indicating a lack of code enforcement and maintenance of the levees. However, there was insufficient information to include maintenance considerations.
3. Impact by a barge, floating debris, or other large object on the floodwalls or levees.
4. Failure of 3-bulb water stops between I-wall sections.

Component Performance

For each component, a performance level was defined such that its occurrence corresponded to a failure to perform an intended function. The critical components within the HPS, as stated above, are the levees, I-walls, T-walls, and transitions and closures. These components can fail in a variety of modes. For each mode of failure a limit state was defined, which, if it were to occur would result in a failure to keep water out of the drainage basin.

Engineering models of the mechanics of component performance are limited in their ability to explicitly model a failure state. As a result, an analysis is usually carried out for incipient failure by examining the limits of stability. If this state is equaled or exceeded, the structure or component is expected to fail to perform as intended. Incipient failure models were usually similar to design calculations, and in many cases were adapted from the GDM's.

For the purpose of evaluating the performance of the levees and floodwalls, *failure* was defined as complete breaching, which allowed water to enter the drainage basin. This failure occurred in two ways: (1) loss of levee or wall stability when the strength of the levee or wall and its foundation was insufficient to withstand the forces placed upon the structure for a given water elevation below the top of the wall or levee (no overtopping); or (2) overtopping caused the protected side of the levee or wall to erode substantially and result in a wall or levee breach, which allowed water to flow freely into the drainage basin.

System Failure

Depending on the performance of individual components in the HPS, various outcomes may result. For purpose of evaluating the performance of the HPS, the outcome of most interest is whether a protected area was flooded or not.

The HPS was assumed to fail if flooding occurred in a protected area, beyond that expected from rainfall and runoff which can be handled by pumping. Given this definition, a failure of the HPS occurred even if the components making up the system did not fail, for example, if levees or walls were overtopped but not breached. Flooding can occur as a result of chains of events occurring individually or in combination. Among these are:

1. Levee or floodwall breaching.
2. Inflow into an area due to levee or flood wall overtopping that does not result in breeching, and which exceeds the capacity of the pumping system.
3. Inflow to an area that occurs as a result of rainfall.
4. Inflow to an area that occurs when the capacity of the pump system is exceeded as a result of backflow through pump houses.

Flooding that occurs as a result of rainfall or transient overtopping in most cases will not be as consequential and may be mitigated by the pumping system.

Fragility curves

Fragility curves summarize the probability of components reaching their respective limit states (i.e., failure), conditioned on levels of water elevation from hurricane conditions. For example, the fragility curve of the probability of failure by deep-sliding instability of a levee section is shown as a function of water height. Design basis water elevation indicates the probability of failure at the design water level (i.e., 3 ft from the top of the levee).

Fragility curves for levees and floodwalls were calculated for two conditions: (1) global stability without overtopping, for which reliability was calculated at two water elevations, design elevation and top of levee, and a smooth curve approximated to lower water elevation at sea level; and (2) overtopping with subsequent erosion, for which reliability was estimated from empirical experience during Katrina at four water elevations of overtopping: ½ foot, 1 foot, 2 feet, and 3 feet above the top of levee or flood wall.

Once the fragility curves for each component failure mode was determined, they were input to the HPS risk model, which is based on event tree analysis. For each sequence in the event tree, a ‘sequence’ fragility curve is determined by evaluating the event tree logic at each successive water elevation level. Once each sequence of events has been evaluated, the composite or total fragility for system failure can be determined for each system performance state of interest (e.g., no flooding has occurred in any area protected by the HPS, or flooding occurred as a result of levee or floodwall failure, or flooding occurred as a result of overtopping) by simply summing the fragility curves for the sequence of events for the same state.

Reliability assessments were performed for individual reaches of approximately homogeneous structural type, elevation, geotechnical conditions, and water elevations. This resulted in fragility curves for each reach by mode of failure. Such fragility curves represented the aleatory (i.e., random) uncertainties from one hurricane to another. These fragility curves were offset to include epistemic uncertainties.

Consequences

One of the primary outputs of the risk and reliability modeling of Risk Team are estimates of the probability distributions of life loss and direct physical damage relating to the performance of the Hurricane Protection System (HPS) in the Greater New Orleans area. The risk was estimated for the following two scenarios:

1. Pre-Katrina (August 28, 2005).
2. Conditions projected for the 2006 Hurricane Season (June 1, 2006).

Risk Team worked in close collaboration with Consequence Team to obtain estimates of life loss and property loss as a function of maximum inundation elevation in the 27 subbasins shown in Figure 1 that comprise the following ten basins of the New Orleans HPS:

East Bank

1. New Orleans Metro - Orleans East Bank
2. New Orleans East
3. St. Bernard Parish
4. Jefferson Parish
5. St. Charles Parish
6. Plaquemines

West Bank

1. Cataouatche
2. Westwego to Harvey Canal
3. Harvey Canal to Algiers Canal
4. Algiers Canal to Hero Canal

The numbers of subbasins that are contained within portions of the following Parishes are indicated in parentheses: Jefferson (7), Orleans (12), Plaquemines (1), Saint Bernard (5), and Saint Charles (2) Parishes.

The Risk Model was run for more than 1,100 different hurricane realizations that represent a wide range of hurricane events with different severities, directions, points of landfall, etc. For each of these hurricane realizations, the Risk Model represented the performance of the HPS and estimated the probability that inundation would result from insufficient internal drainage, overtopping of the levees without breaching, and levee breaching. The resulting estimates of maximum inundation depths were used as a basis for interpolation of life loss and property loss estimates using the relationships that were provided by Consequence Team. Estimates were made for each of the 27 subbasins and for the Pre-Katrina and June 1, 2006 scenarios. Thus it was necessary that the life loss and property loss estimates covered a range of elevations associated with a range of hurricane events that could impact New Orleans from minor inundation to Elevation 36 above sea level.

The estimates of life loss were developed as probability distributions and the estimates of property loss were developed as best estimates with an associated 90% confidence interval rather than single-value or point estimates. The probability distributions for life loss and confidence intervals for property losses represent various types of uncertainties in the estimates.

Uncertainty Analysis

One of the objectives of the risk analysis is to quantitatively assess the uncertainties associated with modeling the performance of the HPS, likelihood of failure and the associated consequences of flooding. There are two fundamentally different sources of uncertainty that affect an estimation of the likelihood of future events. The first is attributed to the inherent randomness of events in nature. These events are predicted in terms of their likelihood of occurring (e.g., the chance of heads in a coin flip). This source of uncertainty is known as aleatory uncertainty and is, in principle, irreducible.

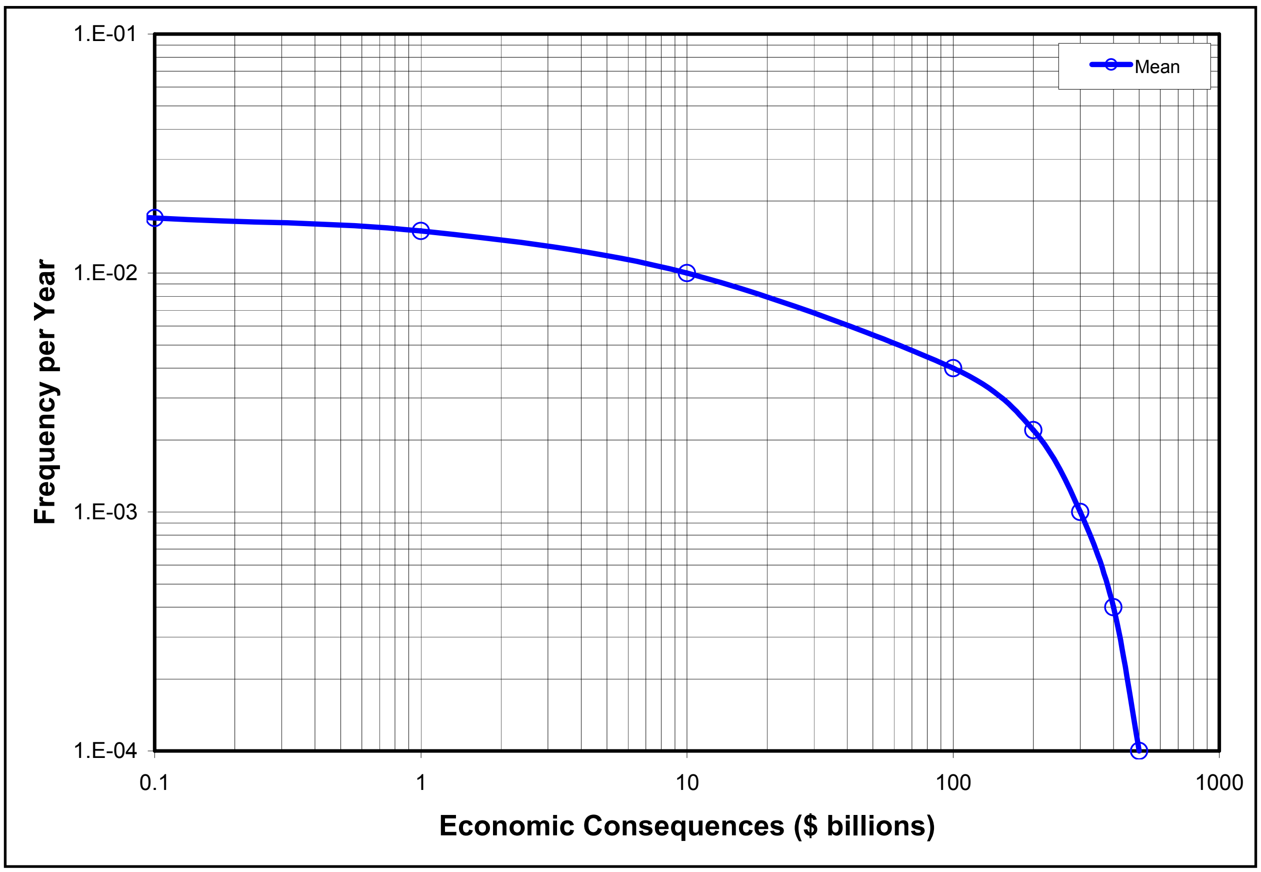

Figure 17. Illustration of Typical Risk Analysis Results for Economic Consequences

The second source of uncertainty is attributed to our lack of knowledge or data. For example, the ability to determine the likelihood of an event (i.e., its rate of occurrence) requires that certain data be available. Depending on the volume of data that is available, the *accuracy* of the estimate of the rate of occurrence will vary. If limited data are available, the estimated rate may be quite uncertain (i.e., statistical confidence intervals on parameter estimates was large). A second type of knowledge uncertainty is attributed to our lack of understanding (e.g., knowledge) about the physical processes that must be modeled (e.g., the meteorological processes that generate hurricane events). Often scientists and engineers have interpretations of existing data and models of physical processes of interest that often competing in the sense they lead to different results, while at the same time are consistent with observations. In these instances expert evaluations are often required to assess the current state of knowledge and to quantitatively evaluate the level of uncertainty. These sources of uncertainty are referred to *as* epistemic (knowledge-based) uncertainty.

The distinction between what is aleatory and what is epistemic uncertainty can often seem arbitrary. For example, the distinction depends on the models that are used in a particular analysis. In addition, their estimates can change in time. Nonetheless, making a distinction between the sources of uncertainty in logical manner helps insure that all uncertainties are quantified and those that was reduced with additional data or knowledge are identified.

In principle, epistemic uncertainties are reducible with the collection of additional data or the use/development of improved models. However, in a given project, it is typically not possible to reduce these uncertainties.

Figure 18 shows an example of where the epistemic uncertainty is manifested in the results of the HPS risk analysis. Shown is the probability density function on the estimate frequency of HPS failure (where failure is simple used here as the occurrence of inundation in one or more protected areas). The uncertainty in the estimate of the frequency of failure is an aggregation of the uncertainties in the estimate of the frequency and magnitude of hurricane storm surge and in the estimate of the reliability (or fragility) of the structures, systems and components that comprise the HPS.

In the HPS risk and reliability analysis, there were uncertainties associated with each of the inputs to the risk model developed by other IPET teams. Sensitivity studies of the parameters used in the drainage model, failure mode models and pumping station performance models are used in order to identify critical sources of uncertainty. In addition, sensitivity studies are conducted during the development of the risk model to identify uncertainties in the input parameters synthesized by Risk Team and to identify data or analyses that could reduce uncertainties.

The effectiveness of the protection system is also dependent upon how well the operational elements of the system performed. Elements such as road closure structures, gate operations and pumping plants, etc. that requires human operation and proper installation during a flood fight can dramatically impact flood levels. The lessons learned concerning the performance of these elements during Katrina was considered in the uncertainty analysis using parametric analysis.

Figure 19 shows the fragility for the HPS including uncertainty and its effect on the estimate of the reliability at the authorization basis.

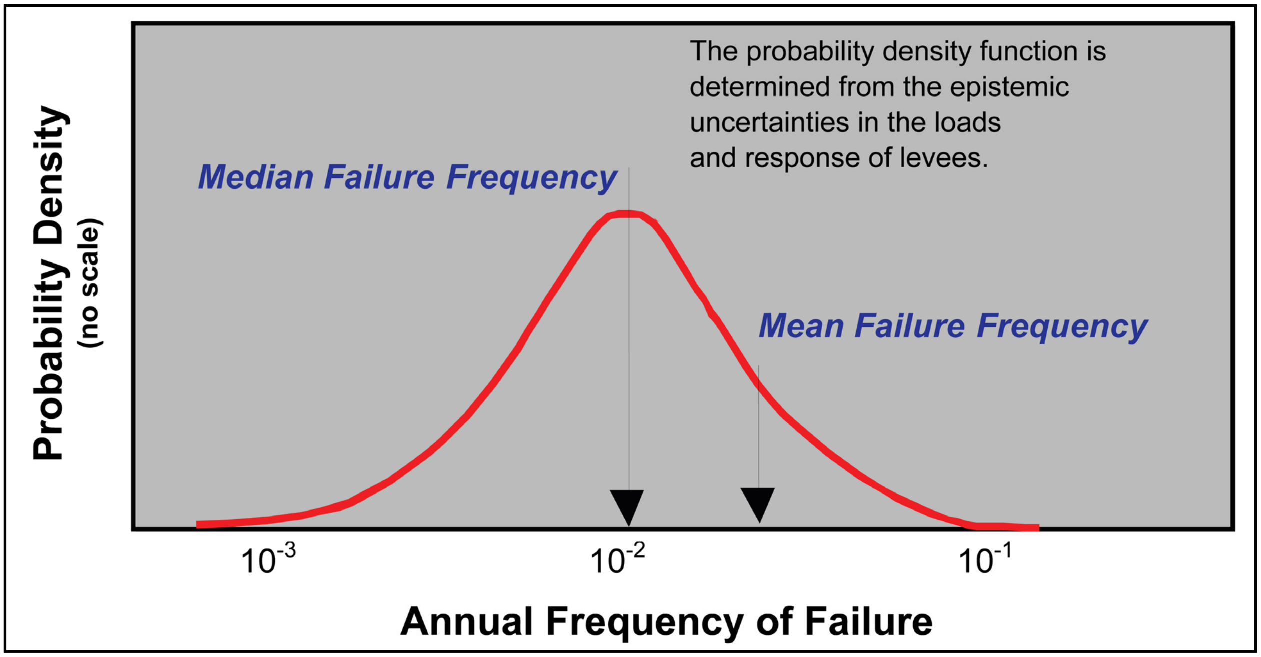

Figure 18. Illustration of the Uncertainty in the Estimate of the Frequency HPS Failure due to Hurricane Events

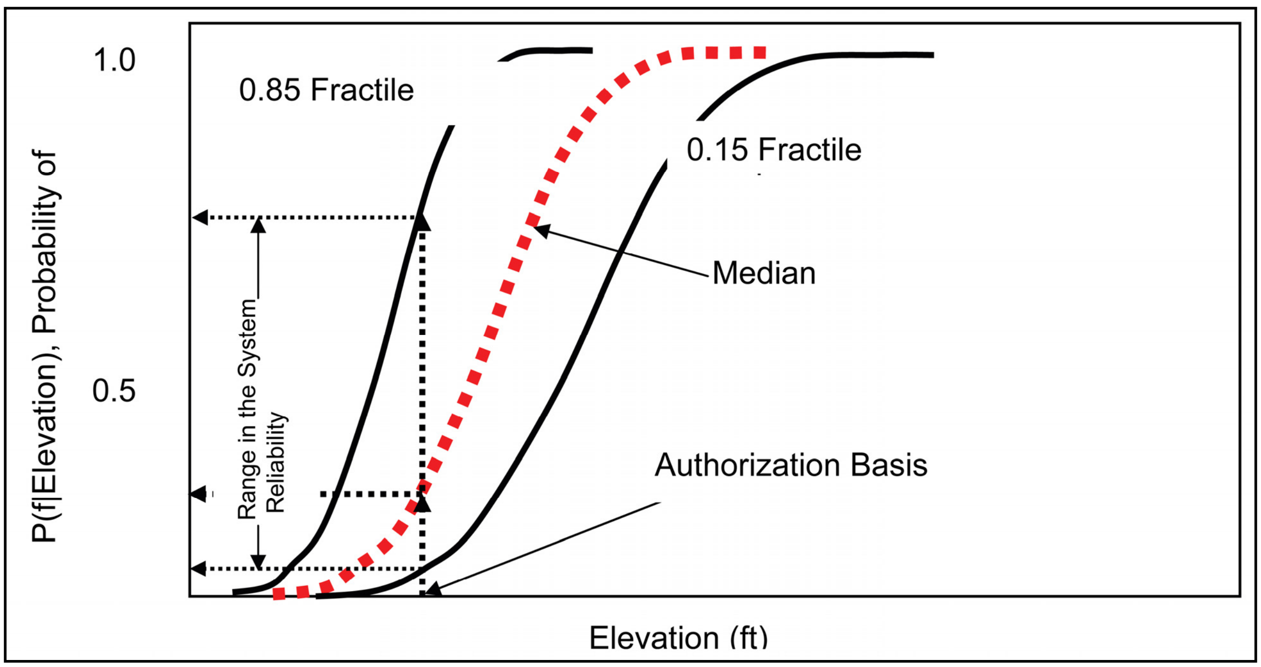

Figure 19. Illustration of the Fragility for the HPS Including Modeling Uncertainty and the Effect at the Authorization Basis

The epistemic uncertainties in each part of the analysis lead to uncertainty in the final risk results. Propagating the uncertainties of the individual parts of the analysis through to the final result, produces a probability distribution on the frequency of exceedance of consequence metrics (e.g., economic consequences). This result is shown in Figure 20.

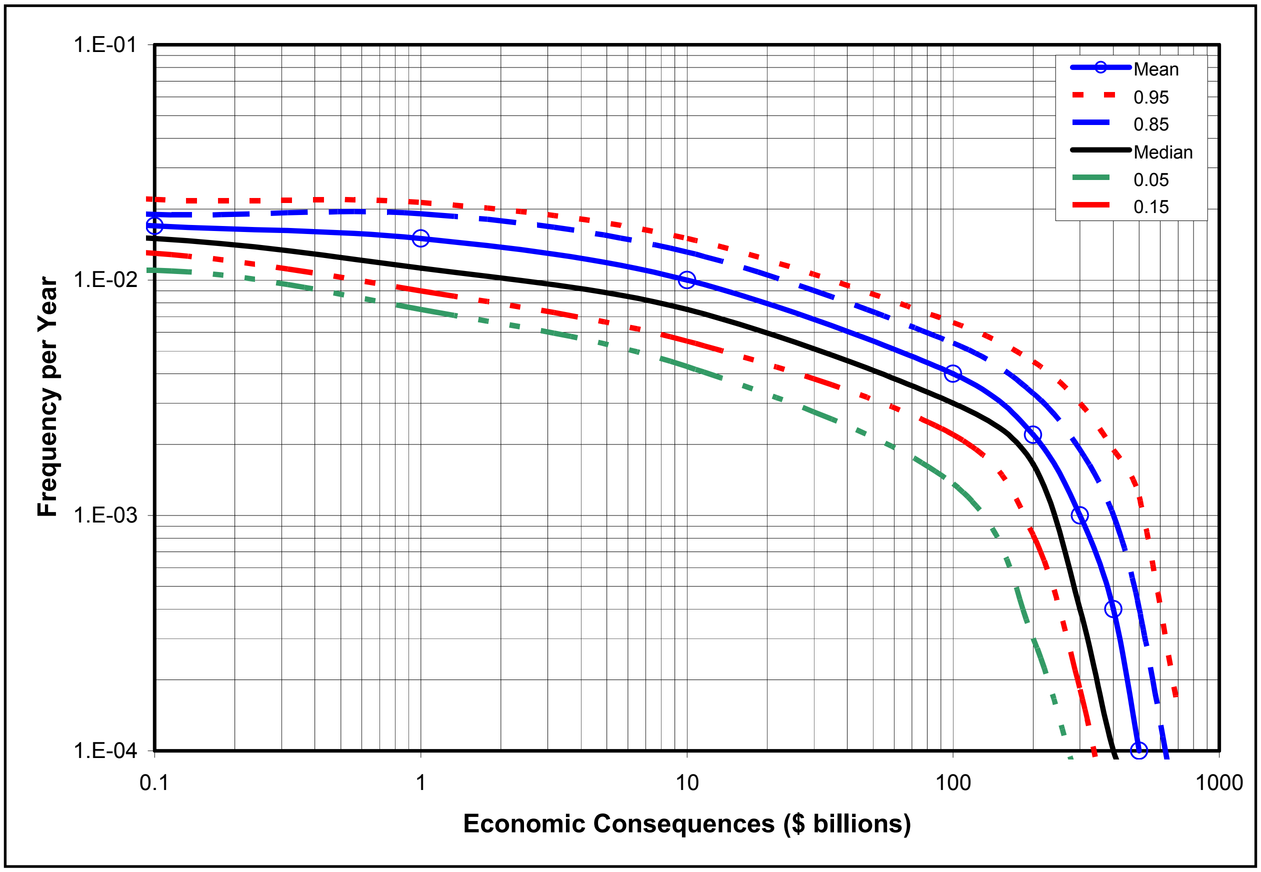

Figure 20. Illustration of Typical Risk Analysis Results for Economic Consequences Including Uncertainty

References

Risk methodology

Ayyub, B. M. 2003. Risk Analysis in Engineering and Economics, Chapman & Hall/CRC Press, FL.

Ayyub, B. M., and McUen, R. H. 2003. Probability, Statistics and Reliability for Engineers and Scientists, Chapman & Hall/CRC Press, FL.

Daugherty, R., Franzini, J., and Finnemore E., 1985, Fluid Mechanics with Engineering Applications, 598 p., McGraw-Hill Book Co., NY.

Kumamoto, H., and Henley, E.J., 1996, Probabilistic Risk Assessment and Management for Engineers and Scientists, Second Edition, IEEE Press, New York.

Modarres, M., Kaminskiy, M., Krivstov, V., 1999. Reliability Engineering and Risk Analysis: A Practical Guide, Marcel Decker Inc., New York, NY.

USACE 2000, Unwatering Plan of the Greater Metropolitan Area of New Orleans, LA, USACE New Orleans District.

Hurricane Methodology

Batts, M. E., Cordes, M. R., Russell, L. R., Shaver, J. R., and Simiu, E. (1980), "Hurricane Wind Speeds in the United States," *Rep. No. BSS-124,* Nat. Bureau of Standards, U.S. Department of Commerce, Washington, D.C.

Bister, M. and K. A. Emanuel (2002), "Low Frequency Variability of Tropical Cyclone Potential Intensity. 1: Interannual to Interdecadal Variability," *J. Geoph. Res.* **107**: 4801.

Broccoli, A. J. and S. Manabe (1990), "Can Existing Climate Models Be Used to Study Anthropogenic Changes in Tropical Cyclone Climate?" *Geophys. Res. Lett.* **17**: 1917-1920.

Chan, J. C. L. and S. L. Liu (2004), "Global Warming and Western North Pacific Typhoon Activity from an Observational Perspective," *J. Climate* **17**: 4590-4602.

Chen, S., M. Lonfat, J. A. Knaff, and F. D. Marks, Jr. (2006), "Effects of Vertical Wind Shear and Storm Motion on Tropical Cyclone Rainfall Asymmetries Deduced from TRMM," submitted to *Monthly Weather Review*.

Chouinard, L. E., C. Liu, and C. K. Cooper (1997), "Model for Severity of Hurricanes in Gulf of Mexico," *J. of Waterway, Port, Coastal and Ocean Engineering,* **123**(3): 120-129.

Elsner, J. B. (2005), "Hurricane Science Review: The Next 5 Years?" Dept. of Geography, Florida State University, *http://garnet.fsu.edu/~jelsner/www*.

Elsner, J. B. and B. Kocher (2000), "Global Tropical Cyclone Activity: A Link to the North Atlantic Oscillation," *Geophys. Res. Lett.* **27**: 129-132.

Emanuel, K. A. (1987), "The Dependence of Hurricane Intensity on Climate," *Nature* **326**: 483-485.

Emanuel, K. A. (2000), "A Statistical Analysis of Tropical Cyclone Intensity," *Mon. Wea. Rev.* **128**: 1139-1152.

Emanuel, K. A. (2005a), "Increasing Destructiveness of Tropical Cyclones Over the Past 30 Years," *Nature* **436**: 686-688.

Emanuel, K. A. (2005b), "Anthropogenic Effects on Tropical Cyclone Activity," Dept. of Earth and Planetary Sciences, MIT, *http://wind.mit.edu/~emanuel/anthro2.htm*.

Free, M., M. Bister, and K. A. Emanuel (2004), "Potential Intensity of Tropical Cyclones: Comparison of Results from Radiosonde and Reanalysis Data," *J. Climate* **17**: 1722-1727.

Georgiou, P. N., Davenport, A. G., and Vickery, B. J. (1983), "Design Wind Speed in Regions Dominated by Tropical Cyclones," *J. Wind Engrg. And Industrial Aerodynamics,* **13**(1): 139-152.

Goldenberg, S. B., C. W. Landsea, A. M. Mestas-Nunez, and W. M. Gray (2001), "The Recent Increase in Atlantic Hurricane Activity: Causes and Implications," *Science* **293**: 474-479.

Haarsma, R. J., J. F. B. Mitchell, and C. A. Senior (1992), "Tropical Disturbances in a GCM," *Climate Dyn.* **8**: 247-257.

Henderson-Sellers, A. H. Zhang, G. Berz, K. A. Emanuel, W. Gray, C. Landsea, G. Holland, J. Lighthill, S-L. Shieh, P. Webster, and K. McGuffie (1998): "Tropical Cyclones and Global Climate Change: A Post-IPCC Assessment," *Bull. Amer. Meteor. Soc.* **79**: 9-38.

Ho, F. P., J. C. Su, J. L. Hanevich. R. J. Smith, and F. P. Richards (1987), "Hurricane Climatology for the Atlantic and Gulf Coasts of the United States," *NOAA Technical Report NWS 38*, U.S. Department of Commerce, Washington, D.C.

Holland, G. J. (1980), "An Analytic Model of the Wind and Pressure Profiles in Hurricanes," *Monthly Weather Review,* **108**: 1212-1218.

Houghton, J. T., Y. Ding, D. J. Griggs, M. Noguer, P. J. van der Linden, and D. Xiaosu, Eds. (2001), Climate Change 2001: The Scientific Basis: Contributions of Working Group I to the Third Assessment Report of the Intergovernmental Panel on Climate Change, Cambridge University Press, 881 pp.

Jarvinen, B. R., Neumann, C. J., and Davis, M. A. S. (1984), "A Tropical Cyclone Data Tape for the North Atlantic Basin 1886-1893: Contents, Limitations and Uses," *NOAA Tech. Memo. NWS-NHC-22,* U.S. Department of Commerce, Washington, D.C.

Knutson, T. R. and R. E. Tuleya (2004), "Impact of CO_2-induced Warming on Simulated Hurricane Intensity and Precipitation: Sensitivity to the Choice of Climate Model and Convective Parameterization," *J. Climate* **17**: 3477-3495.

Landsea, C. W., R. A. Pielke Jr., A. M. Mestas-Nunez, and J. A. Knaff (1999), "Atlantic Basin Hurricanes: Indices of Climatic Changes," *Climatic Change* **42**: 89-129.

Lighthill, J., G. J. Holland, W. M. Gray, C. Landsea, K. A. Emanuel, G. Craig, J. Evans, Y. Kurihara, and C. P. Guard (1994), "Global Climate Change and Tropical Cyclones," *Bull. Amer. Meteor. Soc.* **75**: 2147-2157.

Lonfat, M., F. D. Marks, Jr., and S. S. Chen (2004), "Precipitation Distribution in Tropical Cyclones Using the Tropical Rainfall Measuring Mission (TRMM) Microwave Imager: A Global Perspective," *Mon. Wea. Rev.,* **132**: 1645-1660.

Luettich, R. A., J. J. Westerink, and N. W. Sheffner (1992), "ADCIRC: An Advanced Three-dimensional Circulation Model for Shelves, Coasts and Estuaries; Report 1: Theory and Methodology of ADCIRC-2DDI and ADCIRC-3DL," *Coastal Engineering Research Center, U. S. Army Engineer Waterways Experiment Station,* Technical Report DRP-92-6, Vicksburg, MS.

Michaels, P. J., P. C. Knappenberger, and C. W. Landsea (2005), "Comments on 'Impact of CO_2-induced Warming on Simulated Hurricane Intensity and Precipitation: Sensitivity to the Choice of Climate Model and Convective Parameterization'," *J. Climate,* in press.

Neumann, C. J. (1991), "The National Hurricane Center Risk Analysis Program (HURISK)," *NOAA Tech. Memo. NWS-NHC-38,* U.S. Department of Commerce, Washington, D.C.

Pielke, R. A. Jr., C. W. Landsea, M. Mayfield, J. Laver, and R. Pasch (2005), "Hurricanes and Global Warming," *Bull. Amer. Meteor. Soc.,* November, 2005: 1571-1575.

Powell, M., G. Soukup, S. Cocke, S. Gulati, N. Morisseau-Leroy, S. Hamid, N. Dorst, and L. Axe (2005), "State of Florida Hurricane Loss Projection Model: Atmospheric Science Component," *J. Wind Engineering and Industrial Aerodynamics,* **93**: 651-674.

Russell, L. R. (1971), "Probability Distribution for Hurricane Effects," *J. Wtrwy., Harb. And Coast. Engrg. Div., ASCE,* **97**(1): 139-154.

Scheffner, N. W., L. E. Borgman, and D. J. Mark (1996), "Empirical Simulation Technique Based Storm Surge Frequency Analyses," *J. Wtrwy., Port, Coast., and Oc. Engrg.* **122**(2): 93-101.

Vickery, P. J. and L. A. Twisdale (1995a), "Prediction of Hurricane Wind Speeds in the United States," *J. of Structural Engineering*, **121**(11): 1691-1699.

Vickery, P. J. and L. A. Twisdale (1995b), "Wind-Field and Filling Models for Hurricane Wind-Sped Predictions," *J. of Structural Engineering*, **121**(11): 1700-1709.

Vickery, P. J., P. F. Skerlj, and L. A. Twisdale (2000), "Simulation of Hurricane Risk in the U.S. Using Empirical Track Model," *J. of Structural Engineering*, **126**(10): 1222-1237.

Webster, P. J., G. J. Holland, J. A. Curry, and H.-R. Chang (2005), "Changes in Tropical Cyclone Number, Duration, and Intensity in a Warming Environment," *Science* **309**: 1844-1846.

Willoughby, H. E. and M. E. Rahn (2004), "Parametric Representation of the Primary Hurricane Vortex. Part I: Observations and Evaluation of the Holland (1980) Model," *Monthly Weather Review*, **132**: 3033-3048.

Hurricane Waves

Dally, W. R., R. G. Dean and R. A Dalrymple (1985) "Wave Height Variation Across Beaches of Arbitrary Profile", Journal of Geophysical Research, Vol. 90, No. 6, pp. 11,917 – 11,927.

U.S. Army Corps of Engineers (1984) "Shore Protection Manual", U. S. Government Printing Office, Washington, D. C. Reliability Methodology.

Reliability Modeling

Vanmarcke, E.H. (1977). "Reliability of earth slopes," *Journal of the Geotechnical Engineering Division, ASCE, v.103*(GT11): 1247-1265.

DeGroot, D.J. and Baecher, G.B. (1993). "Estimating autocovariance of in-situ soil properties," *Journal of the Geotechnical Engineering Division, ASCE, v.119*(GT1): 1247-1265.

USACE (1972). "New Orleans East Lakefront Levee Paris Road to South Point, Lake Pontchartrain," Barrier Plan, DM 2 Supplement 5B, New Orleans District, June.